



# A new high-resolution BOLAM-MOLOCH suite for the SIMM forecasting system: assessment over two HyMeX intense observation periods

S. Mariani<sup>1</sup>, M. Casaioli<sup>1</sup>, E. Coraci<sup>1</sup>, and P. Malguzzi<sup>2</sup>

<sup>1</sup>Institute for Environmental Protection and Research (ISPRA), Rome, Italy

<sup>2</sup>Institute of Atmospheric Sciences and Climate (ISAC), Italian National Research Council (CNR), Bologna, Italy

Correspondence to: S. Mariani (stefano.mariani@isprambiente.it)

Received: 30 November 2013 – Published in Nat. Hazards Earth Syst. Sci. Discuss.: 22 January 2014

Revised: 6 October 2014 – Accepted: 21 October 2014 – Published: 5 January 2015

**Abstract.** High-resolution numerical models can be effective in monitoring and predicting natural hazards, especially when dealing with Mediterranean atmospheric and marine intense/severe events characterised by a wide range of interacting scales. The understanding of the key factors associated to these Mediterranean phenomena, and the usefulness of adopting high-resolution numerical models in their simulation, are among the aims of the international initiative HyMeX – HYdrological cycle in Mediterranean EXperiment. At the turn of 2013, two monitoring campaigns (SOPs – Special Observation Periods) were devoted to these issues. For this purpose, a new high-resolution Bologna Limited Area Model-MOdello LOcale (BOLAM-MOLOCH) suite was implemented in the Institute for Environmental Protection and Research (ISPRA) hydro–meteo–marine forecasting system (SIMM – *Sistema Idro-Meteo-Mare*) as a possible alternative to the operational meteorological component based on the BOLAM model self-nested over two lower-resolution domains. The present paper provides an assessment of this new configuration of SIMM with respect to the operational one that was also used during the two SOPs. More in details, it investigates the forecast performance of these SIMM configurations during two of the Intense Observation Periods (IOPs) declared in the first SOP campaign. These IOPs were characterised by high precipitations and very intense and exceptional high waters over the northern Adriatic Sea (*acqua alta*). Concerning the meteorological component, the high-resolution BOLAM-MOLOCH forecasts are compared against the lower-resolution BOLAM forecasts over three areas – mostly corresponding to the Italian HyMeX hydrometeo-

teological sites – using the rainfall observations collected in the HyMeX database. Three-month categorical scores are also calculated for the MOLOCH model. Despite the presence of a slight positive bias of the MOLOCH model, the results show that the precipitation forecast turns out to improve with increasing resolution. In both SIMM configurations, the sea storm surge component is based on the same version of the Shallow water HYdrodynamic Finite Element Model (SHYFEM). Hence, it is evaluated the impact of the meteorological forcing provided by the two adopted BOLAM configurations on the SHYFEM forecasts for six tide-gauge stations. A benchmark for this part of the study is given by the performance of the SHYFEM model forced by the ECMWF IFS forecast fields. For this component, both BOLAM-SHYFEM configurations clearly outperform the benchmark. The results are, however, strongly affected by the predictability of the weather systems associated to the IOPs, thus suggesting the opportunity to develop and test a time-lagged multi-model ensemble for the prediction of high storm surge events.

## 1 Introduction

Forecast verification is an essential activity of any operational institution or centre (dealing with numerical predictions) that arise from the need to constantly assess the skill and value of the forecasts provided by numerical models (see, e.g., Jolliffe and Stephenson, 2011). A statistical verification approach is mandatory to provide a robust and reliable

assessment through time of the system performance, and an evaluation of the impact of any modification introduced in the system (*administrative purpose*: Brier and Allen, 1951). The traditional case study approach is, however, suitable in an operational monitoring and forecasting context, since the assessment of the system performance in predicting significant natural hazard events does not follow directly from statistically based forecast verification over a long time period. A thorough analysis of the key physical features associated to such events is therefore recommended.

Nevertheless, erroneous conclusions on forecast performance could be drawn from case-study verification if the predictability of the weather systems under investigation is not taken into consideration. In particular, focusing on cyclones producing high-impact weather over the Mediterranean (Jansa et al., 2014), highly predictable atmospheric processes, such as large synoptic disturbances undergoing Alpine lee cyclogenesis (see, e.g., Speranza et al., 1985), and much less predictable atmospheric processes, such as moist cyclogenesis in presence of complex orography (see, e.g., Romero, 2011), can give rise to similar patterns producing the same kind of ground effects. Numerical weather prediction (NWP) models provide for the former, and not for the latter, correct and timely early warning. This arises from the intrinsic physical properties of the involved weather systems, rather than the NWP model skill.

The necessity to enhance the knowledge (and to assess the predictability) of high-impact atmospheric and marine events in the Mediterranean Basin, and to properly resolve the scales involved that range from synoptic to the meso-gamma scale, led to the establishment at the beginning of the 21st century of the “HYdrological cycle in Mediterranean EXperiment” (HyMeX, <http://www.hymex.org/>; Drobinski et al., 2014). By involving a large number of technical and scientific experts from the meteorological, hydrological, and oceanographic communities, this international collaborative initiative endorsed by the World Meteorological Organization intends to improve over one decade (2010–2020) the observation and modelling strategy needed for monitoring and predicting high-impact events, such as high precipitation events, flash floods, intense air–sea exchanges, and dense water formation. Two Special Observation Period (SOP, <http://sop.hymex.org/>) campaigns were carried out at the end of 2012 (5 September–6 November) and at the beginning of 2013 (February–March) to investigate, in selected target areas, the key physical processes leading to such high-impact events by providing detailed and dedicated (e.g., using instrumented aircrafts) observations (Ducrocq et al., 2014).

An ad hoc forecasting activity (Ducrocq et al., 2014; Ferretti et al., 2014) based on several numerical model forecasts was set up during each SOP to identify in advance the Intense Observation Periods (IOPs) to be monitored. For this specific activity, the Institute for Environmental Protection and Research (ISPRA) provided the meteorological products of its operational hydro–meteo–marine forecasting system called

*Sistema Idro-Meteo-Mare* (SIMM; see Sect. 2.1; Speranza et al., 2004, 2007; Mariani et al., 2014). The SIMM meteorological component consists of a parallel version of the hydrostatic Bologna Limited Area Model (BOLAM, Buzzi et al., 1994; Malguzzi and Tartaglione, 1999), developed by the Institute of Atmospheric Sciences and Climate (ISAC) of the Italian National Council of Research (CNR), self-nested over two domains. In addition, a new forecasting configuration of SIMM was implemented and used during the HyMeX SOPs (see Sect. 2.2). This was obtained by replacing the BOLAM self-nesting with a higher-resolution meteorological suite based on an improved BOLAM version and the non-hydrostatic model called MODello LOcale (MOLOCH; Malguzzi et al., 2006).

Nine out of sixteen IOPs monitored during the first SOP campaign affected the three Italian HyMeX hydrometeorological sites (North-Eastern Italy (NEI), Liguria–Tuscany (LT), and Central Italy (CI)). Among these, IOP16 (25–29 October 2012) and IOP18 (31 October–1 November 2012) deserved particular attention. Although the weather systems associated with these IOPs were rather different from a synoptic point of view (and, hence, in terms of predictability), they displayed some similarity in terms of ground effects, producing heavy precipitation over the NEI, LT and CI sites and intense storm surge events over the northern Adriatic coastline and the Venice Lagoon (the so-called *acqua alta* events; see Sects. 3 and 4). This latter aspect is particularly relevant due to the national role of ISPRA in monitoring and forecasting hydrological and hydrographic parameters over the Venice Lagoon. Thus, the two IOPs are used to test the improvement, if any, in replacing the lower-resolution BOLAM configuration with the new higher-resolution BOLAM-MOLOCH suite, and to assess the performance of the SIMM storm-surge forecasting component, namely the Shallow water HYdrodynamic Finite Element Model (SHYFEM, Umgiesser et al., 2004; Bajo et al., 2007; Zampato et al., 2007).

The paper is organised as follows. The description of the operational SIMM and of the HyMeX-based SIMM is depicted in Sect. 2. Section 3 provides the synoptic description of IOP16 and IOP18. Forecast verification results for both the meteorological and sea storm surge components of the two analysed configurations of SIMM are presented in Sect. 4. Conclusions and final remarks are reported in Sect. 5.

## 2 Overview of the operational and the HyMeX-based SIMM configurations

### 2.1 The operational SIMM

The first chain considered, the operational SIMM, is a quite recent upgraded configuration of the chain originally implemented in 2000 and later updated for the meteorological component in 2009 (Speranza et al., 2007; Mariani et al.,

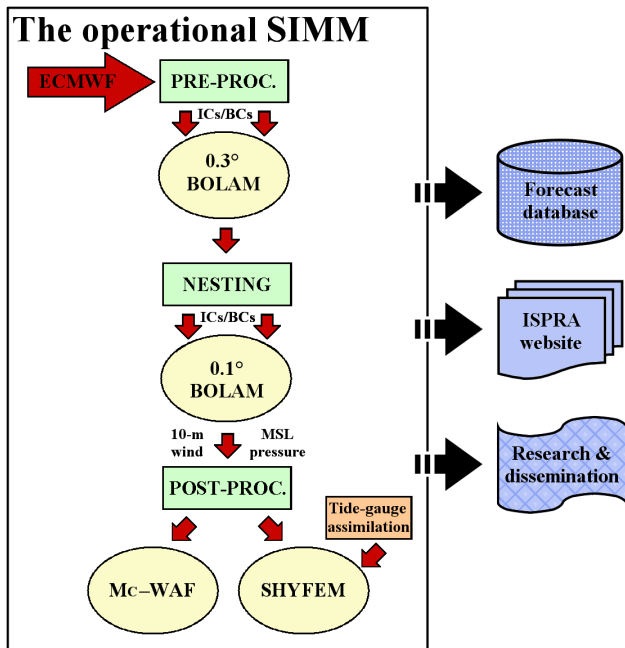


**Figure 1.** A sketch of the general processing scheme for the operational SIMM: from the ECMWF forcing to the storage, online publication and use for research and dissemination of weather, marine and coastal products. The operational configuration includes the BOLAM meteorological model nested at 0.3 and 0.1°, with a 0.5° ECMWF forcing, the Mc-WAF wave modelling suite forced by the 0.1° BOLAM, and the low/high-resolution SHYFEM sea surge model forced by the 0.1° BOLAM (and ECMWF – not shown), with and without a tide-gauge assimilation process.

2014). This chain adopts the 2009 version of the hydrostatic BOLAM meteorological model and two new components for the wave and storm surge forecasts (see Fig. 1).

The operational SIMM is initialised on a daily basis by means of 0.5° analyses and forecasts provided by the 12:00 UTC run from the previous day of the European Centre for Medium-Range Weather Forecasts (ECMWF) Integrated Forecasting System (IFS). The set of initial and boundary conditions (ICs/BCs) includes, for a 96 h forecast range, the 3-D geopotential height, temperature,  $u$  and  $v$  wind components, and specific humidity over 15 isobaric levels and the 2-D surface temperature, snow depth, and first-level soil temperature.

BOLAM is one-way nested over two domains (Fig. 2) covering the Mediterranean basin, with horizontal spatial size equal to 0.3° (33 km) and to 0.1° (11 km), to provide daily meteorological forecast fields. Every day, the “father” model produces 96 h coarse-resolution forecasts starting from 12:00 UTC of the previous day, whereas the “son” model produces 84 h high-resolution forecasts ([http://www.isprambiente.gov.it/pre\\_meteo/](http://www.isprambiente.gov.it/pre_meteo/)) starting from 00:00 UTC (from +12 to +96 h). The first 12 h of the father run are neglected as a spin-up time period.

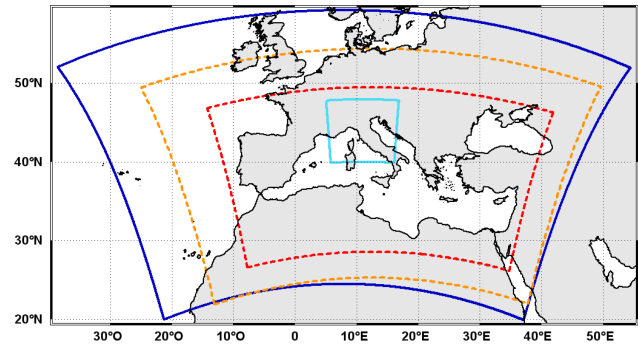


**Figure 2.** Computational domains for the meteorological component of the operational SIMM, namely the 0.3° BOLAM (orange long-dashed line) and the 0.1° BOLAM (red long-dashed line), and of the HyMeX-based SIMM, namely the 0.07° BOLAM (blue solid line) and the 0.0225° MOLOCH (sky blue solid line).

The 0.1° BOLAM surface wind fields are then post-processed to be used for feeding the Mediterranean-embedded Costal Wave Forecasting system (Mc-WAF, Inghilesi et al., 2012). The Mc-WAF component adopts the 3rd generation Wave Model (WAM, The Wamdi Group, 1988) to analyse the large-scale, deep-sea propagation of surface waves in the Mediterranean Sea, and the Simulating Waves Nearshore model (SWAN, Booij, 1999; The SWAN Team, 2014) to simulate waves in several Italian coastal areas ([http://www.isprambiente.gov.it/pre\\_mare/coastal\\_system/maps/first.html](http://www.isprambiente.gov.it/pre_mare/coastal_system/maps/first.html)). Regional intermediate-scale WAM grids are also introduced to bridge the gap between the large scale and coastal areas. The reader is referred to Casaioli et al. (2014) for a full account of the regional and coastal areas implemented into Mc-WAF.

Simultaneously, the 0.1° BOLAM wind and mean sea level pressure forecast fields are used to force the new storm surge forecasting component that predicts the sea surface elevation in the Mediterranean Sea and, in particular, in the northern Adriatic Sea (<http://www.venezia.isprambiente.it/modellistica>). This component is based on the shallow-water model SHYFEM developed at the Institute of Marine Sciences (ISMAR) of CNR. SHYFEM is also forced with the wind and mean sea level pressure fields generated from ECMWF IFS at 00:00 UTC, providing this way an cost-effective multi-model forecasting system for the *acqua alta* prediction.

Two finite-element grids for the Mediterranean Sea are used in SHYFEM for both the BOLAM and IFS initialisation: a low-resolution grid with 13 180 elements (Table 2 and Fig. 3); and a high-resolution grid with 50 409 elements (Table 2). For each grid, the operational system carries out a first run to predict the storm surge contribution over the entire Mediterranean, followed by a second run to calculate the total water level, that is, the astronomical tide added to

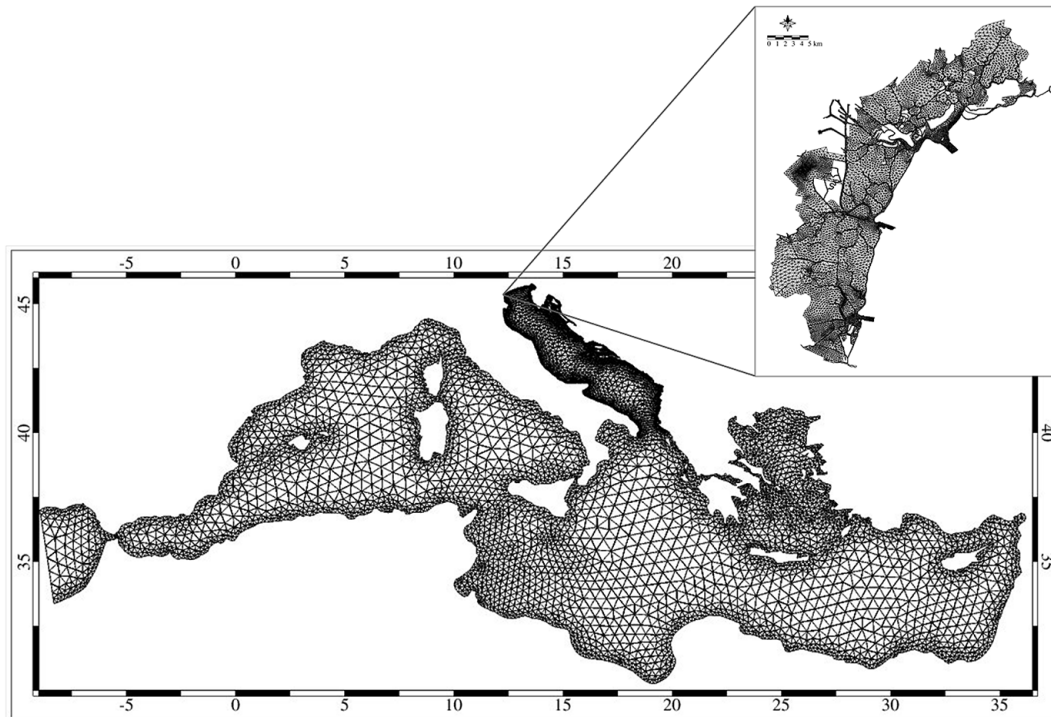


**Figure 3.** The SHYFEM low-resolution finite-element grid, with a zoom over the Venice Lagoon. After <http://www.venezia.isprambiente.it/modellistica>.

the storm surge contribution (or tidal residual)<sup>1</sup>, only in the Venice Lagoon. The total water level extracted at the CNR Acqua Alta oceanographic platform (hereinafter referred to as Piattaforma; Cavaleri, 1999), situated 8 nautical miles off the Venice coast, is applied as BC to the lagoon inlets for the second run to provide the total sea level forecast in the main lagoon locations. In order to avoid a long spin-up period, the state vector of the dynamic system is saved, for each simulation, into a restart file (Bajo et al., 2007). This is then used as IC of the next-day forecast simulation (Table 1).

A data assimilation module based on the 4-D physical space assimilation system is also present (Bajo et al., 2012) for integrating the residual sea level measurements from the tide gauges of the ISPRA observation network located alongside the Italian northern Adriatic coastline (hereinafter referred to as RMLV – see for more details <http://www.venezia.isprambiente.it/rete-meteo-mareografica>). This module is, however, still under development and testing.

## 2.2 The HyMeX-based SIMM

A newer configuration of the SIMM forecasting chain was designed for the HyMeX campaigns. The new chain, depicted in Fig. 4, differs from the operational one for using the higher-resolution BOLAM-MOLOCH suite in place of lower-resolution, two-domain nested BOLAM configuration.

<sup>1</sup>The storm surge contribution includes here the seiches, as well.

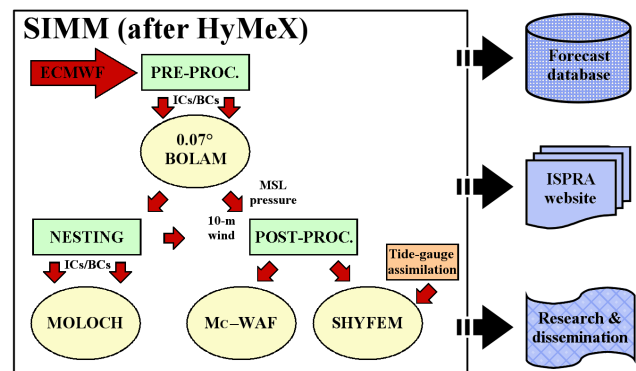


**Figure 4.** As in Fig. 1, but for the SIMM configuration (not yet operational) designed for the HyMeX campaigns. This configuration includes the BOLAM meteorological model nested at 0.07°, with a 0.25° ECMWF forcing, the 0.0225° MOLOCH forced by BOLAM, the Mc-WAF wave modelling suite forced by BOLAM and MOLOCH, and the low- and high-resolution SHYFEM sea surge model forced by BOLAM, with and without a tide-gauge assimilation process.

The BOLAM configuration adopted within this suite is based on a newer version (dated 2012) of the numerical code and uses a wider domain, covering an area 54–25° N and from 18° W to 43° E (see Fig. 2), with a grid mesh size of 0.07° (7.8 km). In addition, the 0.25° ECMWF analyses and forecasts are directly applied as ICs/BCs to BOLAM without

**Table 1.** Schematic description of the principal model settings of the operational SIMM and the HyMeX-based SIMM.

System	Component	Model	Grid spacing	ICs/BCs (Lead time)	Additional forcing	Forecast range	Permitting convection	Assimilation
Operational SIMM	Meteorological	BOLAM	0.3°	0.5° ECMWF IFS (12:00 UTC of day-1)	–	84 h (+12 to +96 h)	No	No
	Wave (Mc-WAF)	WAM	1/30°	0.3° BOLAM (00:00 UTC)	–	84 h		
		SWAN	1/240°	SWAN of day-1 (00:00 UTC)	Wind fields from 0.1° BOLAM	84 h	–	No
	HyMeX-based SIMM	Sea storm surge		Low-res. finite-element grid (see Table 2)	ICs from SHYFEM of day-1; no BCs (00:00 UTC)	Wind and MSLP fields from 0.5° ECMWF IFS	96 h	–
SHYFEM			High-res. finite-element grid (see Table 2)					
Meteorological		BOLAM	0.07°	ICs from SHYFEM of day-1; no BCs (00:00 UTC)	Wind and MSLP fields from 0.1° BOLAM	84 h	–	Yes or No
		MOLOCH	0.0225°	0.25° ECMWF IFS (12:00 UTC of day-1)	–	48 h (+12 to +60 h)	No	No
Wave (Mc-WAF)	WAM	1/30°	007° BOLAM (00:00 UTC)	–	48 h	Yes		
	SWAN	1/60°	WAM of day-1 (00:00 UTC)	Wind fields from 0.07° BOLAM and/or 0.025° MOLOCH	48 h	–	No	
		1/240°	SWAN of day-1 (00:00 UTC)					
	Sea storm surge	SHYFEM	Low-res. finite-element grid (see Table 2)	ICs from SHYFEM of day-1; no BCs (00:00 UTC)	Wind and MSLP fields from 0.07° BOLAM	48 h	–	Yes or No
			High-res. finite-element grid (see Table 2)					

**Table 2.** Parameters of the low- and high-resolution finite-element grids of SHYFEM.

Finite-element grid	Number of grid points	Mediterranean Basin		Adriatic Sea		Venice Lagoon	
		Min	Max	Min	Max	Min	Max
Low-resolution	13 180	15 km	60 km	5 km	30 km	50 m	800 m
High-resolution	50 409	8 km	40 km	2 km	15 km		

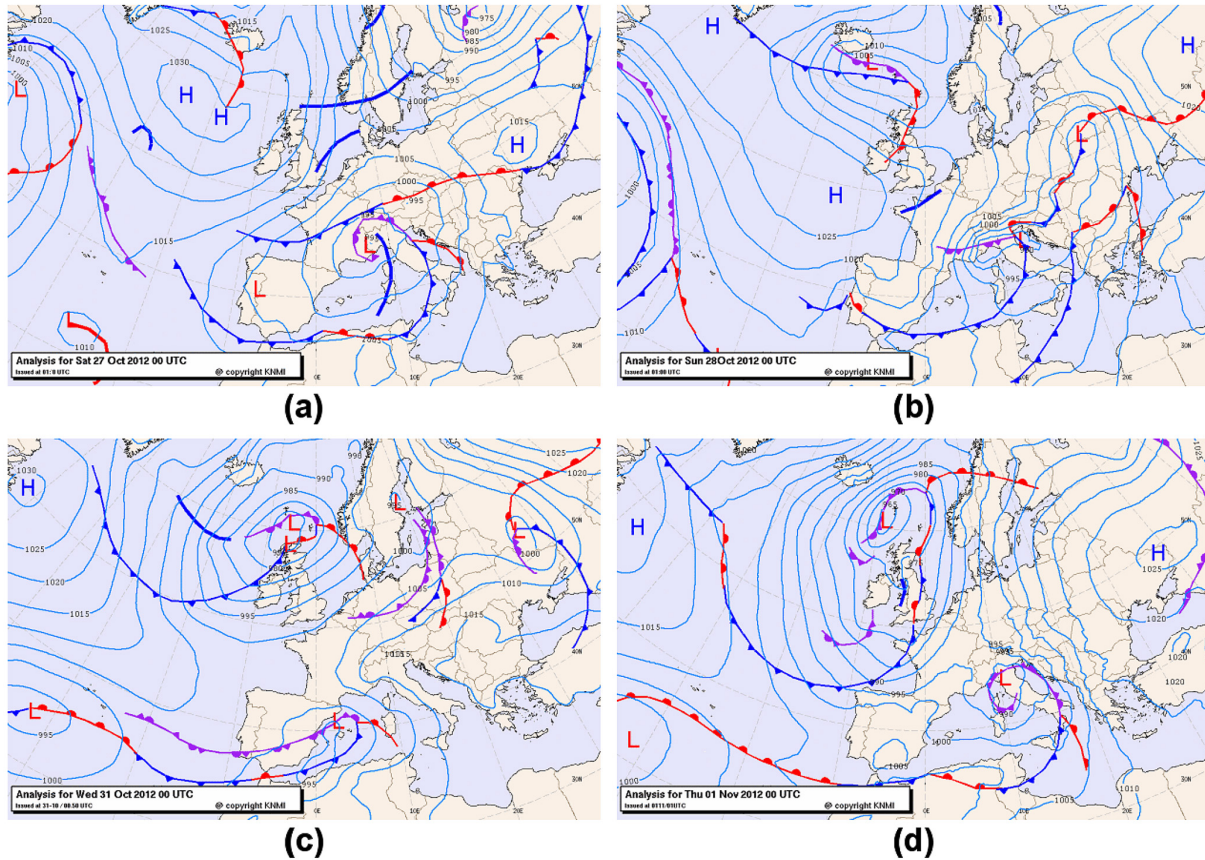


**Figure 5.** Synoptic analysis charts at 00:00 UTC. Upper panels for IOP16: (a) 27 October 2012; (b) 28 October 2012. Lower panels for IOP18: (c) 31 October 2012; (d) 1 November 2012. Courtesy of the Royal Netherlands Meteorological Institute (KNMI).

using a coarser-resolution father model run. Unlike the operational initialisation set (see Sect. 2.1), this higher-resolution IC/BC set contains the 2-D logarithm of surface pressure in place of the 3-D geopotential height. It also includes the 3-D temperature,  $u$  and  $v$  wind components, specific humidity, and cloud water and ice over 46 (out of the 137 available) hybrid levels, temperature and water content of the first four ECMWF soil levels, and the 2-D skin temperature, land-sea mask, orography, and land use. The forecast range of this initialisation set is 60 h.

The non-hydrostatic MOLOCH model is then nested into the  $0.07^\circ$  BOLAM run to produce higher-resolution forecasts over the domain shown in Fig. 2, with a grid mesh size of  $0.0225^\circ$  (2.5 km), mainly covering northern and cen-

tral Italy. This domain was chosen to include at least five of the eight hydrometeorological sites monitored during the HyMeX SOPs. When the new chain will be operational, the MOLOCH domain will cover the entirety of Italy, approximately  $49\text{--}34^\circ$  N and  $5\text{--}25^\circ$  E. Both BOLAM and MOLOCH runs start at 12:00 UTC of the previous day (given that the 12:00 UTC ECMWF run is used) and last 60 h. The first 12 h are not considered (and indeed they were not provided to the SOP campaigns). When operational, the forecast range of the BOLAM-MOLOCH suite will be extended from 48 to 84 h.

The wind fields modelled by the BOLAM-MOLOCH suite are then used for initialising Mc-WAF (see Casaioli et al., 2014), whilst only the  $0.07^\circ$  BOLAM wind and mean sea

level pressure fields are considered for forcing SHYFEM over both the low- and high-resolution finite-element grids.

### 3 The HyMeX IOP16 and IOP18: synoptic analysis and ground effects

During the IOP16, a large Atlantic cyclone crossed the Iberian Peninsula on 25–26 October. Then, it moved rapidly eastwards, reaching on 27 October the Genoa Gulf (Fig. 5a), where it was reinforced and made almost stationary by the phenomenon of Alpine cyclogenesis during the next day (Fig. 5b). Finally, it left Italy on 29 October. Observations of the weather system development were provided by several operational and specifically deployed instruments, including ground meteorological networks, radiosondes, and ground- and satellite-based remote-sensing instruments. In the morning of 27 October, an instrumented SAFIRE Falcon 20 aircraft was additionally used to obtain airborne measurements over the CI site. These data were collected into the HyMeX database (<http://mistrals.sedoo.fr/HyMeX/>) and they are now available for research studies.

The event occurred during the IOP18 was characterised by the formation of a Mediterranean low-level cyclone over the Gulf of Lion on 31 October (Fig. 5c), embedded in the zonal flow connected to an upper-level trough (not shown). Subsequently, the cyclone moved along a similar path of the IOP16 one (Fig. 5d). The difference between the two events was mainly in the time and space scale of the dynamical and physical processes involved. This, in turn, reflected in a different predictability of the two weather systems. Also in this case, several detailed and specific observations were collected in order to monitor and study the key processes responsible for this event.

Both events produced intense precipitation over Italy, with some similarity in the rainfall patterns. The precipitation over the Italian HyMeX hydrometeorological sites, and also over southern Italy, was associated with southerly low-level advection of warm and moist air and subsequent frontal passage.

Over LT, strong advection of warm and moist air over steep and complex orography acted in both cases to concentrate intense precipitation in very small areas. Over CI, the key factor was the prediction of the development of multiple squall lines over the Tyrrhenian Sea, embedded in the warm and unstable south-westerly flux. These arose in several precipitation bands over peninsular Italy, whose exact space-time location was hard to predict. Over NEI, the two IOP events are typical examples of the so-called “dark Bora” phenomenon, that is, a cyclonic Bora wind with cloudy sky and precipitation (Jurčec, 1981). A warm south-easterly Scirocco wind flowing over the Adriatic Sea swerved westwards (following the classical Bora NE–SO wind direction), due to the barrier effect jointly produced by the Dalmatian orography and the cold, stable air present over the north-eastern Ital-

ian region during the passage of the occluded front. This phenomenon, matching the astronomical tide, was also responsible for the *acqua alta* events in the Venice Lagoon (for IOP18, see Crosato, 2012).

The evolution of these tidal events was monitored through the national RMLV network. At the Punta della Salute tide gauge, the sea level exceeded twice the warning level during IOP16 (more than 120 cm), whilst it exceeded once the alarm level during IOP18 (143 cm at 00:40 UTC of 1 November). According to historical records, the latter peak represents the 16th maximum tidal level observed in Venice at Punta della Salute since 1872. The same meteorological event was responsible of a tide peak<sup>2</sup> of 164 cm in Chioggia Vigo, a town to the south of Venice, which represents the maximum observed value since 1990 for this station. Also in Grado, north-east of Venice, a peak<sup>2</sup> of 137 cm was measured in the early morning of 1 November.

### 4 Forecast verification and model intercomparison

Each operational modelling component of SIMM has been objectively evaluated during the entire lifetime of the system (see, e.g., [http://www.isprambiente.gov.it/pre\\_meteo/pub.html](http://www.isprambiente.gov.it/pre_meteo/pub.html) for a compendium of the forecast verification activities). The introduction of significant modifications in the chain structure and/or in the models has been always preceded by a rigorous forecast verification analysis to assess the impact on the system performance of such modifications. This was also done for the new high-resolution configuration of BOLAM used in the HyMeX-based SIMM, before its deployment in the two SOP campaigns.

The 0.07° BOLAM version was statistically evaluated against alternative BOLAM configurations in a study fully described in a paper by Casaioli et al. (2013). A multi-method approach was adopted that included also the calculation of several categorical scores. It was demonstrated that the 0.07° BOLAM statistically performs better than the alternative BOLAM configurations and, in particular, the 0.1° BOLAM present in the operational SIMM. Thus, the following part of this work (see Sects. 4.1 and 5) focuses only on the performance of the different SIMM NWP models in predicting the key features associated with IOP16 and IOP18. In addition, for the MOLOCH model, a forecast evaluation in terms of categorical scores is provided since this specific model configuration has not yet been statistically verified.

The assessment of the Mc-WAF component during the two HyMeX SOP campaigns was presented by Casaioli et al. (2014) in a distinct paper due to the complexity of this modelling component that spans from the Mediterranean to local coastal scales using, for its initialisation, the

<sup>2</sup>Value expressed with respect to the mean sea level computed by averaging the observations of sea level in Punta della Salute carried out over 25 years, from 1885 to 1909, and setting the central year (1897) as a reference value.

meteorological fields provided by both the currently operational ( $0.1^\circ$  BOLAM) and the HyMeX-based ( $0.07^\circ$  BOLAM +  $0.0225^\circ$  MOLOCH) SIMM chains. The comparison between the significant wave heights, predicted and observed at some locations of the ISPRA national wind wave buoy network (<http://www.telemisura.it/>), shows an improvement at regional scale when Mc-WAF is initialised with the wind fields modelled by the  $0.07^\circ$  BOLAM rather than the  $0.1^\circ$  BOLAM. This is also true for the skill of Mc-WAF in predicting the two severe events with significant wave height around 3–4 m occurred during IOP16 and IOP18.

Concerning SHYFEM, Cordella (2013), Ferla (2013), and Coraci (2014) computed, for the northern Adriatic Sea, the impact on forecast performance of the different meteorological forcing (BOLAM vs. IFS) used within the operational SIMM. These studies considered 1 year of simulations – from October 2012 to October 2013 – that included mostly of the two SOPs. Although the performances are generally good and quite similar over the considered period, the BOLAM-forced SHYFEM overperforms the IFS-forced SHYFEM when considering high tide events ( $> 80$  cm) and longer lead times. The following Sect. 4.2 provides a comparison of the two SHYFEM configurations that belong, respectively, to the operational SIMM and the HyMeX-based SIMM. Since the latter configuration is not yet fully operational, the comparison is here available only for the period covering the IOP16 and IOP18. In addition, the comparison does not consider the simulations obtained by deploying the data assimilation scheme that is currently under development.

## 4.1 Precipitation forecast

### 4.1.1 Statistical assessment

A quantitative precipitation comparison for a period covering both IOPs (25 October–1 November 2012; see Fig. 6) is suitable to assess the overall forecast performance of the three NWP models. For this purpose, attention is focused on the three Italian HyMeX hydrometeorological sites.

First, hourly rainfall data provided by Italy to the HyMeX database were considered and accumulated on a daily basis starting from 00:00 UTC. Similarly, hourly precipitation forecast fields were accumulated from 00:00 to 24:00 UTC (i.e., +12 to +36 h from the ECMWF initialisation time). Then, observed and modelled daily precipitation amounts were averaged over three intense rainfall areas in LT (lon:  $8.75$ – $11.25^\circ$  E; lat:  $43.8$ – $44.8^\circ$  N, Fig. 6a); CI (lon:  $11.7$ – $13.9^\circ$  E; lat:  $45.3$ – $46.7^\circ$  N, Fig. 6b); and NEI (lon:  $10.5$ – $13.0^\circ$  E; lat:  $41.5$ – $43.0^\circ$  N, Fig. 6c).

In the majority of cases, the  $0.1^\circ$  BOLAM predicts more rainfall than the  $0.07^\circ$  BOLAM, with MOLOCH in an intermediate position. Consistently, the highest observed peaks discussed above – on 26 October over LT and on 31 October over NEI – are best matched by MOLOCH, overestimated

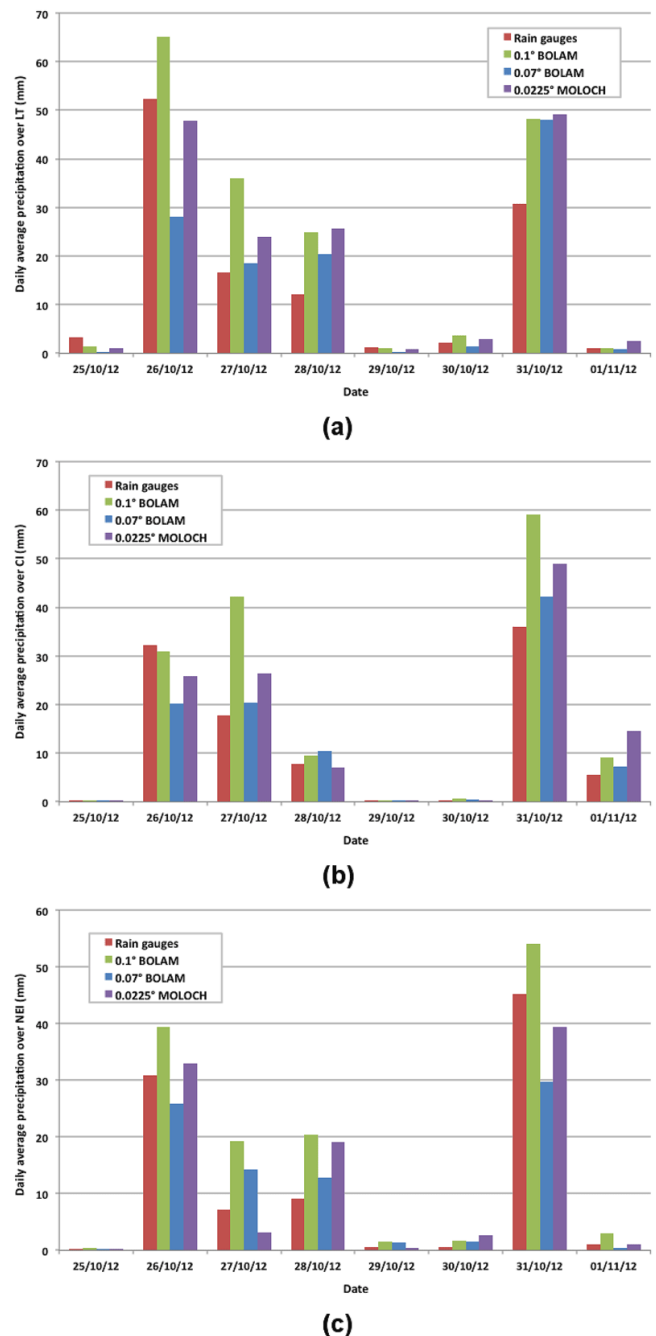


**Figure 6.** Comparison between the daily rainfall observations and the daily precipitation fields generated by the tree inter-compared meteorological models. The time series are averaged over three selected areas: (a) LT; (b) CI; and (c) NEI.

by the  $0.1^\circ$  BOLAM, and underestimated by the  $0.07^\circ$  BOLAM. The IOP18 rainfall over LT is overestimated by the three models to the same extent.

In addition, a statistically robust verification was performed for MOLOCH by assessing the quantitative precipitation forecast (QPF) performance over the period September–

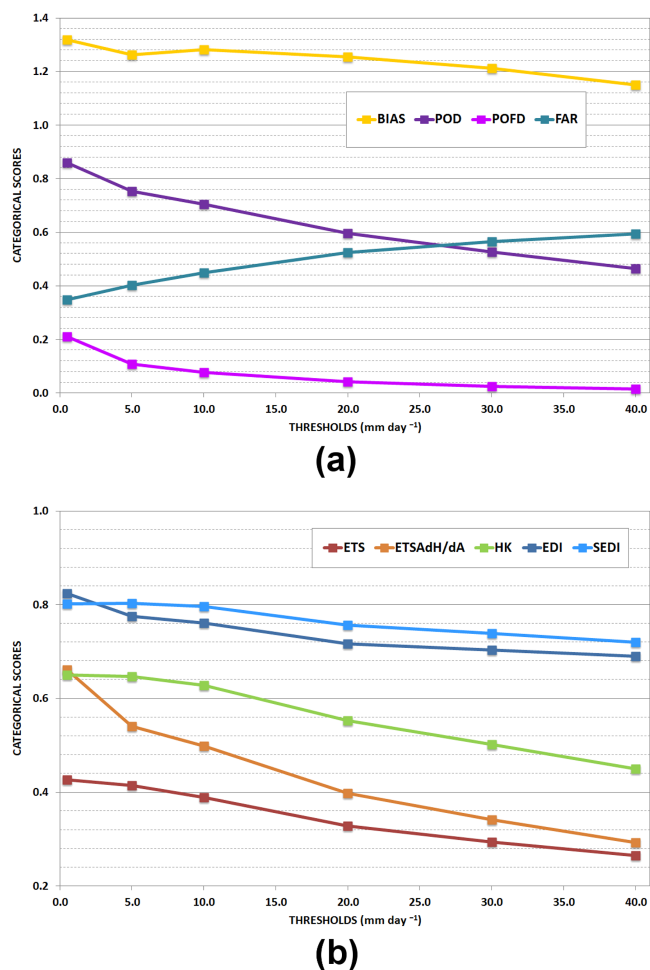


**Figure 7.** Categorical scores calculated over the period September–December 2012 for the 24 h MOLOCH forecasts. (a) BIAS, POD, POFD, and FAR; (b) ETS, ETSAdH/dA, HK, EDI, and SEDI.

December 2012 that includes the first SOP devoted to the monitoring of high precipitation events. The QPF comparison focused on the entire MOLOCH domain (see Fig. 2). Hence, observations from rain gauge networks of Austria, Bosnia and Herzegovina, Croatia, France, Italy, Slovenia, and Swiss were considered.

Several categorical scores were calculated (Fig. 7): the frequency bias (BIAS), the probability of detection (POD), the probability of false detection (POFD), the false alarm ratio (FAR), the equitable threat score (ETS), a bias-adjusted ETS (ETSAdH/dA), the Hanssen–Kuipers score (HK), the extreme dependency index (EDI), and the symmetric extreme dependency index (SEDI). These scores were also adopted for the more recent performance assessment of the BOLAM configurations deployed in ISPRA (Mariani et al., 2014; Casaioli et al., 2013). The score calculation is based on a sum of  $2 \times 2$  contingency tables that summarise the match and mismatch between a series of precipitation observation-forecast pair

above (and below) a selected threshold (see, e.g., Jolliffe and Stephenson, 2011). Six rainfall thresholds were considered, namely 0.5, 5.0, 10.0, 20.0, 30.0, and 40.0 mm 24 h<sup>-1</sup>.

Before populating the contingency tables, both observations and forecasts were accumulated on a daily basis from 06:00 to 06:00 UTC. This time period was chosen to include into the verification observational analysis those Croatian and Slovenian rainfall data that were already 24 h accumulated over this time slot when stored in the HyMeX database. The observed and forecast fields were up-scaled over a common 0.05° lon–lat regular verification grid, mostly covering the MOLOCH domain. This was done to reduce the effect on categorical scores of the double penalty error that can be excessively penalising when verifying very-high resolution forecasts (see, e.g., Rossa et al., 2008; Gilleland, 2013).

A detailed description of the verification procedure and of the various tools used can be found in Mariani et al. (2014).

Over the 3-month period and the up-scaled verification domain, the MOLOCH configuration tends to overpredict the occurrence of precipitation events since a BIAS value slightly greater than one is obtained for all thresholds (Fig. 7a). In other words, the number of false alarms – that is, the rainfall events predicted but not observed – is not negligible and it is greater than the number of observed rainfall events not detected (i.e., the misses). This is a signal that MOLOCH, although providing more realistic precipitation patterns, tends to produce an excess of rainfall. It is also remarkable that BIAS lightly decreases for increasing thresholds.

In Fig. 7a the FAR values provide a quantification of the fraction of events forecast but not observed. Since for a perfect forecast system FAR should be equal to zero, it is even clearer that, for this configuration of MOLOCH, the number of false alarms is not negligible. It could be surprising that the trend of FAR does not follow that of BIAS, but this is the consequence of the fact that, unlike the latter, the former does not take into account the number of misses in the verification sample. The other two scores present in Fig. 7a are POD and POFD that measure, respectively, the fraction of events observed that were correctly forecast and the fraction of no-events (observations below the threshold) that were incorrectly forecast. For a perfect forecast system, POD (POFD) should be equal to one (zero). MOLOCH shows higher POD values at the lower thresholds. For the higher thresholds, there is a decrease of the number of events observed that were properly predicted. The values of POFD are very low and quite close to zero, due to the magnitude of the no-events (i.e., observations and forecasts both below the considered rainfall threshold) with respect to the false alarms.

The MOLOCH skill scores are reported in Fig. 7b. A perfect forecast system has all skill scores equal to one. Each one of these scores assesses a different attribute of the forecast quality and some of them are more (e.g., ETS) or less sensitive (e.g., ETSAdH/dA) to the forecast bias. As for the scores in Fig. 7a, skill scores tend generally to degenerate to

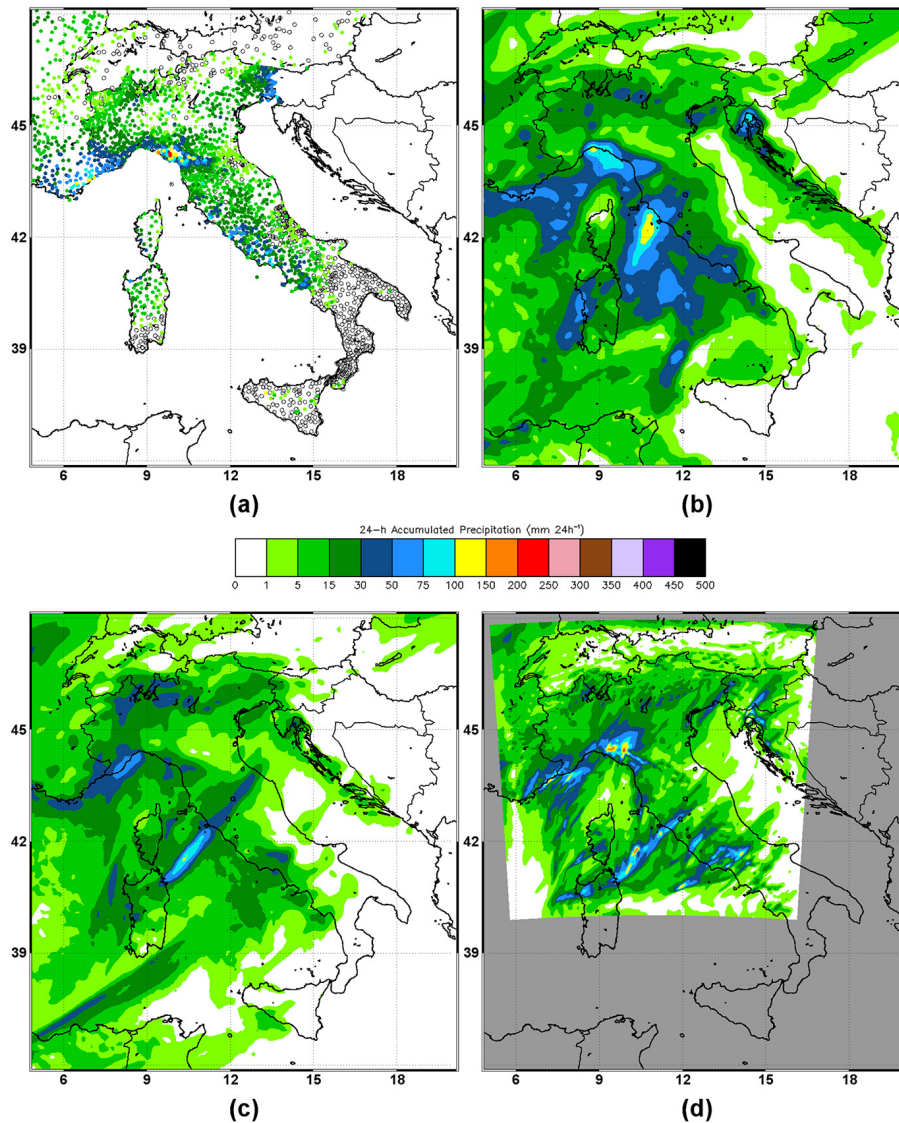


**Figure 8.** 24 h accumulated precipitation on 26 October 2012. Focus over Italy: (a) rain gauge observations; (b)  $0.1^\circ$  BOLAM forecast from the operational SIMM; (c)  $0.07^\circ$  BOLAM forecast from the HyMeX-based SIMM; (d)  $0.0225^\circ$  MOLOCH forecast from the HyMeX-based SIMM (where the area external to the model domain is shaded in grey). The forecasts were initialised at 12:00 UTC of 25 October.

trivial values at high precipitation thresholds, with the exception of EDI and SEDI that have been recently introduced in literature to assess the model skill in forecasting rare, low-base rate precipitation events. An ETS value greater/equal to 0.4 is found for low thresholds, while a value around 0.3 is attained at the medium and higher thresholds. When the effect of bias is removed in the  $ETS_{dH/dA}$  computation, the system turns out to perform better especially at the lower thresholds (where the model is more biased – see Fig. 7a). In terms of HK that, unlike ETS, measures the model accuracy in correctly forecasting both events (i.e., observations and forecasts both above the considered rainfall threshold) and no-events, MOLOCH scores better with values always greater than 0.45 and close to 0.65 at the lower thresholds.

Finally, EDI and SEDI calculated over the re-calibrated forecasts (i.e., bias removed), show that there is no significant difference in the model performance between the thresholds associated with low-base rate rainfall events and those associated with high-base rate.

At this stage, it is not possible to judge how satisfying these scores are since no other MOLOCH configurations were previously implemented in SIMM. Moreover, a direct comparison with the two hydrostatic BOLAM configurations is unfair due to the significant differences in the spatial scales resolved. Higher-resolution NWP models produce detailed forecast fields that contain differing degrees of small-scale details. Such forecasts could score worse than smoother fields modelled by lower-resolution NWP models due to the

sensitivity of categorical scores to small displacement errors (“double penalty” – see, e.g., Mass et al., 2002; Weygandt et al., 2004; Lanciani et al., 2008; Gilleland, 2013).

In the framework of the HyMeX Science Team “Studies of IOPs (SOP1) – precipitation events”, an intercomparison study is ongoing for evaluating the forecast performance of the different NWP models used during the first SOP. This includes the assessment of the ISPRa 2.5 km MOLOCH against the two MOLOCH configurations operational at CNR-ISAC, having horizontal grid spacing of 1.5 and 2.3 km (see Table 4 in Ferretti et al., 2014). According to preliminary results (not shown), no big differences in score were found among the three MOLOCH configurations, except for a (slightly) larger tendency of the ISPRa configuration to overpredict the occurrence of rainfall events (i.e.,  $\text{BIAS}_{\text{ISPRa-MOLOCH}} \geq \text{BIAS}_{\text{ISAC-MOLOCHs}}$ ). This BIAS difference may have, nonetheless, a non-negligible impact on the QPF intercomparison (see Mariani et al., 2014 and references therein). Thus, the sensitivity of the MOLOCH categorical scores to the BIAS, as well as the BIAS difference due to the different choice of ICs/BCs (12:00 UTC ECMWF IFS run vs. 00:00/18:00 UTC GFS runs), different configurations of the parental model, and different extension of the model domains, are currently under investigation.

#### 4.1.2 Case studies

During IOP16, intense precipitation over Italy occurred in two phases. On 26 October, warm and moist south-westerly advection towards Liguria and CI created the favourable conditions to the development of pre-frontal convective cells (Fig. 8a). Particularly intense rainfall occurred over Liguria due to orographic triggering. The rain gauge in Piana di Battolla (see red dots in Fig. 8a) registered  $245 \text{ mm } 24 \text{ h}^{-1}$  (with a maximum of  $45 \text{ mm h}^{-1}$ ). Meanwhile, south-easterly moist advection (Scirocco) on the Adriatic Sea produced convective rain over NEI. On 27 October (not shown), more rainfall affected the Apennines (including LT, with a maximum of  $168 \text{ mm } 24 \text{ h}^{-1}$ ) during the passage of the cold front. At the same time, the eastern Alps chain triggered intense moist convection on the eastern border of NEI and western Slovenia, where 194 mm were registered in 24 h (Nova Gorica).

An overall comparison of the 24 h accumulated precipitation fields predicted on 26 October by the three meteorological models (initialised at 12:00 UTC of 25 October; Fig. 8b–d) evidences a strong similarity in the rain/no-rain patterns with relevant differences in the small-scale details, including the maximum precipitation amount. In particular, the rainfall peak observed in Liguria (Fig. 8a) is misplaced by the  $0.1^\circ$  BOLAM (from the operational SIMM, Fig. 8b), while precipitation over the same area is underestimated by the  $0.07^\circ$  BOLAM forecast (from the HyMeX-based SIMM, Fig. 8c). However, MOLOCH forced by the  $0.07^\circ$  BOLAM displays a very good agreement with observations (Fig. 8d).

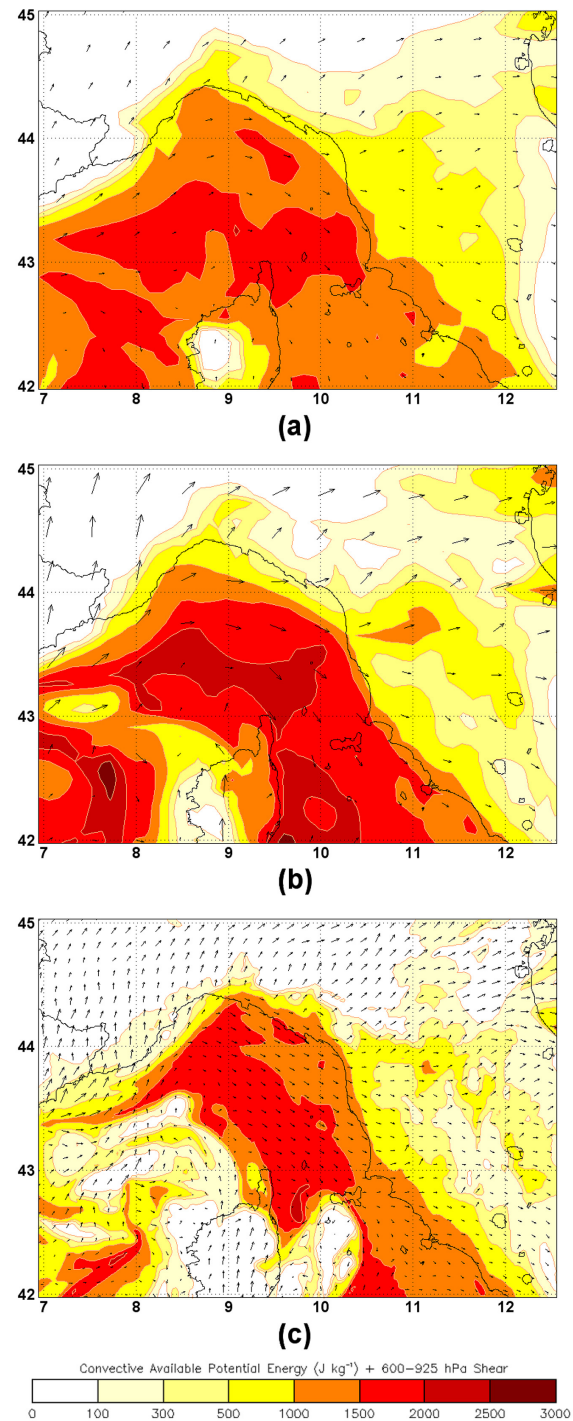


**Figure 9.** Contour plot of the CAPE forecast at 15:00 UTC of 26 October 2012 over the LT hydrometeorological site and 600–925 hPa shear for the  $0.1^\circ$  BOLAM from the operational SIMM (a), and the  $0.07^\circ$  BOLAM (b) and the  $0.0225^\circ$  MOLOCH (c) from the HyMeX-based SIMM. The forecasts were initialised at 12:00 UTC of 25 October.

In particular, the two main rainfall peaks 30 km apart – the western one observed during the morning, the eastern one during the afternoon – are well resolved and correctly estimated (not shown). Similarly, the 0.1° BOLAM provides over CI a better estimate of the rainfall amount than the 0.07° BOLAM, but the latter is more accurate in localising the atmospheric structures. As a consequence, the MOLOCH forecast is able to correctly reproduce the observed multiple band rain pattern (even if with some spatial errors). Finally, the NEI event is hardly visible only in the MOLOCH forecast.

On 27 October, all the three models are able to correctly forecast the location of the rainfall patterns over the HyMeX hydrometeorological sites (not shown). In this case, the 0.1° BOLAM tends to overestimate the rainfall amounts, while the 0.07° BOLAM underestimates the rainfall peaks and MOLOCH gives the best forecast.

A further analysis of the LT event allows the aforementioned forecast differences to be clarified. The CAPE forecast fields at 15:00 UTC of 26 October (Fig. 9) illustrate the situation leading to heavy precipitation on a very small area in the subsequent hours (westernmost red dots on Liguria in Fig. 8a). There, a persistent southerly low-level jet on the eastern Genoa Gulf advects moist, unstable air on the steep orography, generating a long-lasting stationary convective cell. The unstable low-level jet is evident as a high-CAPE area in all three forecasts. A low-CAPE area is present west of Corsica in the 0.07° BOLAM forecast (Fig. 9b) and it is even more developed in the nested MOLOCH run (Fig. 9c), but it is almost absent in the 0.1° BOLAM forecast (Fig. 9a), possibly due to lack of detail in the IC fields. The comparatively better performance of MOLOCH does not arise from such differences: actually, it seems more linked to the main role of the small-scale orographic forcing in this case.

During IOP18, rainfall affected the same Italian areas (Fig. 10a). On 31 October, south-westerly and southerly moist-advection-induced orographic precipitation over the Lazio Region and LT with isolated peaks of more than 140 and 120 mm 24 h<sup>-1</sup>, respectively. Over NEI, convective squall lines developed on 31 October into the Scirocco flow over the northern Adriatic Sea, subsequently hitting the coast and further developing over the mainland. High precipitation over Veneto and Friuli Venezia Giulia Regions was observed during the evening of 31 October. Finally, a big convective cell developed over Trieste in the first hours of 1 November, associated with the passage of the occluded front (not shown).

Most of the features observed in the complex precipitation pattern of Fig. 10a are caught by the three models for this IOP (initialised at 12:00 UTC of 30 October, Fig. 10b–d). In particular, with respect to the 0.1° BOLAM (Fig. 10b), the 0.07° BOLAM (Fig. 10c) partly fixes the rainfall underestimation over LT and the overestimation over NEI and southern Italy, while, at the same, it introduces some rain underestimation over CI.

Details added in the rainfall pattern by the MOLOCH forecast (Fig. 10d) seem to be realistic, even if their verification requires a deeper inspection of the NEI event alone, in view of its relationship with the severe *acqua alta* episode described in Sect. 4.2. According to all models (Fig. 11), a strong, E–W low-level convergence line develops in the last hours of 31 October, deviating the southerly Scirocco moist flow towards the Po Valley as a combined result of the Alpine range barrier effect and the upstream cyclonic vorticity. The convergence line triggers convection over the Veneto Region and, at a later stage, upwind the eastern Alps. The increase in model resolution (Fig. 11a–c) acts to sharpen the convergence line without affecting its evolution, so that the predicted precipitation patterns turn out rather similar.

It must be noted that the IOP18 forecast depends critically on ICs. For instance, if the forecast is initialised one day earlier, that is, at 12:00 UTC of 29 October, the 24 h accumulated precipitation on 31 October turns out to be largely overestimated, and the position of the maximum rainfall over NEI turns out to differ in the two BOLAM and in the MOLOCH simulations (not shown). More specifically, this manifestation of chaos affects the evolution of the mesoscale cyclone (and the associated surface winds) developing over the Mediterranean Sea, with relevant implications on the prediction of the sea storm surge in the Venice Lagoon and the northern Adriatic Sea with more than 2 days in advance (as shown later in Sect. 4.2). Figure 12 illustrates this point through the comparison of the EUMETSAT Meteosat Second Generation (MSG) 6.2 μ water vapour (WV) channel image against the 0.07 and 0.1° BOLAM forecast patterns of the 1.5 PVU potential vorticity (PV) isosurface height. The ECMWF-IFS 500 hPa geopotential analysis and the 0.07 and 0.1° BOLAM 500 hPa geopotential height (GPH) and 300 hPa wind fields are added for reference to the EUMETSAT image and to the BOLAM forecasts, respectively.

Two subsequent 0.1° BOLAM runs (initialised with the ECMWF-IFS runs at 12:00 UTC of 29 and 30 October, respectively) and the correspondent 0.07° BOLAM runs are checked at 00:00 UTC of 1 November, corresponding with the maximum sea surge in Venice. As highlighted by the red ellipses in the figure panels, the position, orientation, size, and intensity of the cyclone clearly display sensitivity to both ICs and choice of model configuration. Instead, the same study performed for the evolution of the IOP16 weather system displays a much more stable and accurate model performance (not shown).

## 4.2 Tidal forecast

Further elements on the performance of the two SIMM configurations in predicting low-probability/exceptional storm surge events can be provided by assessing the SHYFEM forecasts for IOP16 and IOP18. The verification study presented in this section deals with the SHYFEM model forced using the meteorological fields provided by the 0.1° BOLAM

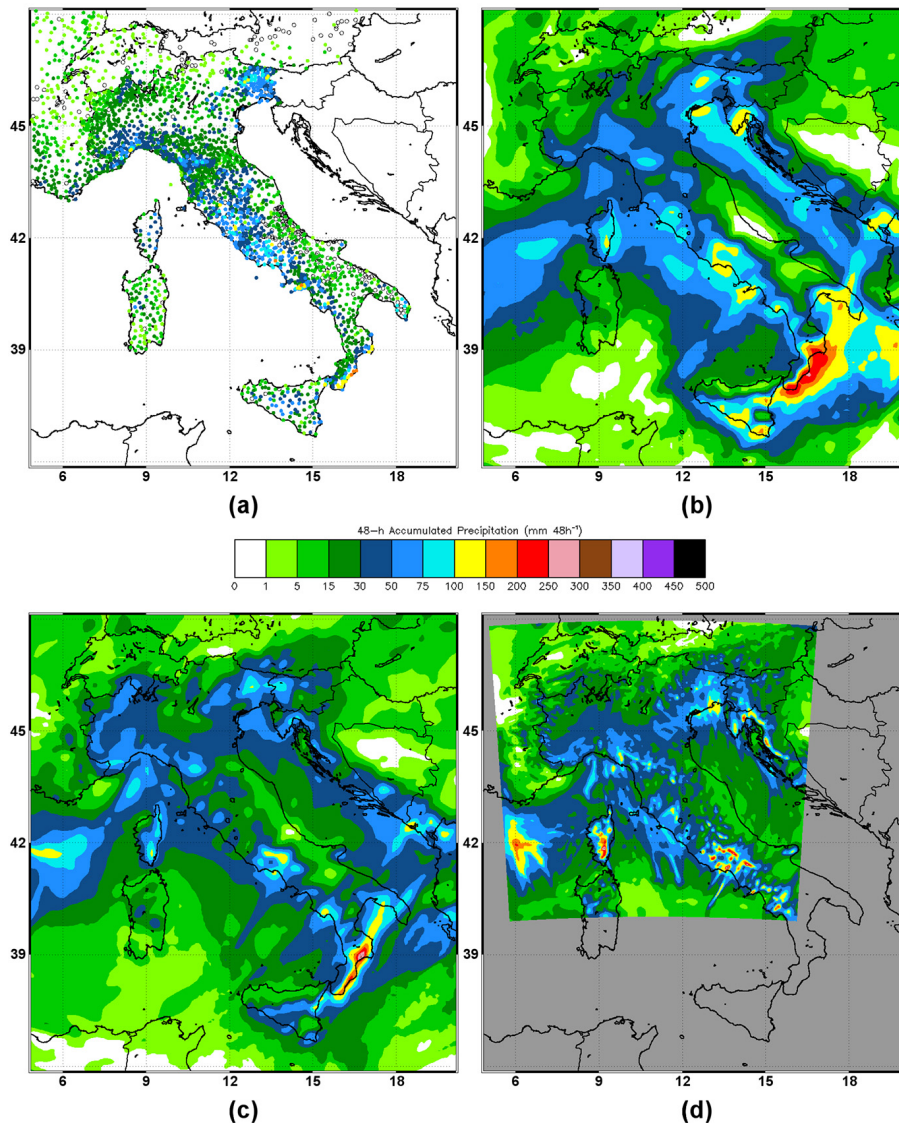


**Figure 10.** As in Fig. 8, but for the 48 h accumulated precipitation starting at 00:00 UTC of 31 October 2012. The forecasts were initialised at 12:00 UTC on 30 October.

from the operational SIMM and the  $0.07^\circ$  BOLAM from the HyMeX-based SIMM, as well as by the  $0.5^\circ$  ECMWF IFS (see Table 1 for the configuration details).

The SHYFEM simulations considered here refer to the period that goes from the beginning of IOP16 to the end of IOP18. Since each daily simulation spanned for several days (see “forecast range” in Table 1), observations were compared against SHYFEM forecasts with different lead times (i.e., the time from the run initialisation) to study the forecast sensitivity to ICs. In the rest of this section, the SHYFEM simulations are then referred with respect to the delivery date, and plotted accordingly in Figs. 14–17 (i.e., different colours correspond to different delivery date).

The use of MOLOCH in combination with SHYFEM will be the subject of a subsequent verification study. For this

purpose, the new domain covering the entirety of Italy (see Sect. 2.2) must be considered; the MOLOCH domain used in the HyMeX configuration is too small to correctly drive the surge model.

The simulations of the three model configurations were checked against observations taken at six different tide-gauge stations. Five of them, from the ISPRA RMLV network, are located in the Venice Lagoon: namely Burano, Punta della Salute, Torson di Sotto, Faro Rocchetta, and Chioggia Vigo. The sixth one is the Venice Municipality tide gauge placed at the CNR Piattaforma. These locations have been chosen among the 23 measuring points available in the Venice Lagoon – together with the open-sea CNR platform – in order to provide a cross-shaped sample of the variability of both observed and forecast sea levels along and across the lagoon

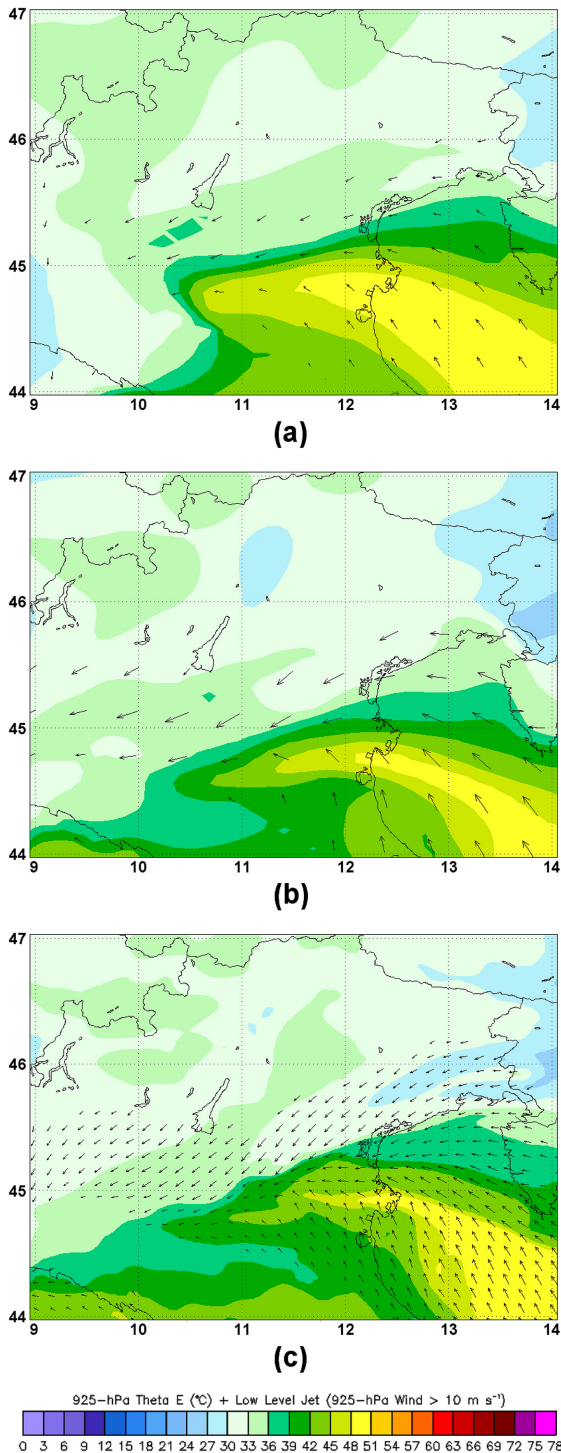


**Figure 11.** Contour plot of the 925 hPa ( $\theta_e$ ) forecast at 21:00 UTC of 31 October 2012 over the NEI hydrometeorological site and the low-level jet forecast for the 0.1° BOLAM from the operational SIMM (a), and the 0.07° BOLAM (b) and the 0.0225° MOLOCH (c) from the HyMeX SIMM. The forecasts were initialised at 12:00 UTC of 30 October.

(Fig. 13). Since it was found that the grid resolution had a negligible effect on the SHYFEM performance for these events (not shown), only the results obtained with the high-resolution SHYFEM configurations are discussed here.

Concerning IOP16, all the model configurations provide a good tidal forecast, both in open-sea (Fig. 14a, c, e) and in the lagoon (Fig. 14b, d, f, for Punta della Salute), with a correlation coefficient varying from 0.89 to 0.97 depending on lead time, meteorological forcing and measuring station.

For the ECMWF IFS-forced SHYFEM configuration, the latest delivered forecast of the 28 November peak is very good. In all the other cases, this configuration tends to underestimate the elevation peaks of an amount that, as it could be expected, is minimum for the shortest-lead time run (see Fig. 14a and b). This error is mostly absent in the forecast forced by the 0.1° BOLAM (Fig. 14c and d), which provides a very accurate estimate of the two maxima in most of the stations (not shown). As an exception, the second peak in Piattaforma is overestimated by the shortest lead-time run (Fig. 14c). The 0.07° BOLAM-driven SHYFEM forecast (Fig. 14e and f) introduces some further improvements, removing the overestimation error visible in the Piattaforma forecast (see Fig. 14c vs. e) and providing more stable forecasts for increasing lead time. However, the 0.07° BOLAM partly reintroduces in Punta della Salute the underestimation error found on ECMWF-driven runs (Fig. 14f).

The behaviour of the SHYFEM configurations during the IOP18 event is by far more complex. Let us start with the description of the results obtained with the forcing provided by the ECMWF-IFS meteorological fields (Fig. 15). Along with an overall tendency of the SHYFEM runs to underestimate the main peaks, a sort of anomalous behaviour is found in relation with the forecast quality when increasing the lead time (hereinafter referred as to the *lead time anomaly*). In general, it is expected that the more recent the meteorological forcing is, the better the forecast is. Here the opposite behaviour is found in most cases. For instance, at Piattaforma (Fig. 15c) or at Faro Rocchetta (Fig. 15d), forecast quality increases slightly but progressively with increasing lead time. Similarly, northwards (Fig. 15a and b) the forecast delivered on 28 October (the oldest one) is much more skilful than the three most recent ones. Regarding the second peak (around 07:30 UTC at Piattaforma and 09:00 UTC at Punta della Salute), the latest forecast delivered on 31 October is the best but, again, the oldest one, delivered on 28 October, is more accurate than that delivered on 29 October. It is also remarkable that the forecast tendency to underestimate the sea surge increases progressively from north (Burano, Fig. 15a) to south (Chioggia, Fig. 15e). This error is hereinafter referred to as the *north/south lagoon unbalance*.

The results from the BOLAM-driven SHYFEM runs (Figs. 16 and 17 for the low- and high-resolution case, respectively) display a general increase of forecast quality. However, they are prone to lead time anomaly and north/south lagoon unbalance, although at a different extent

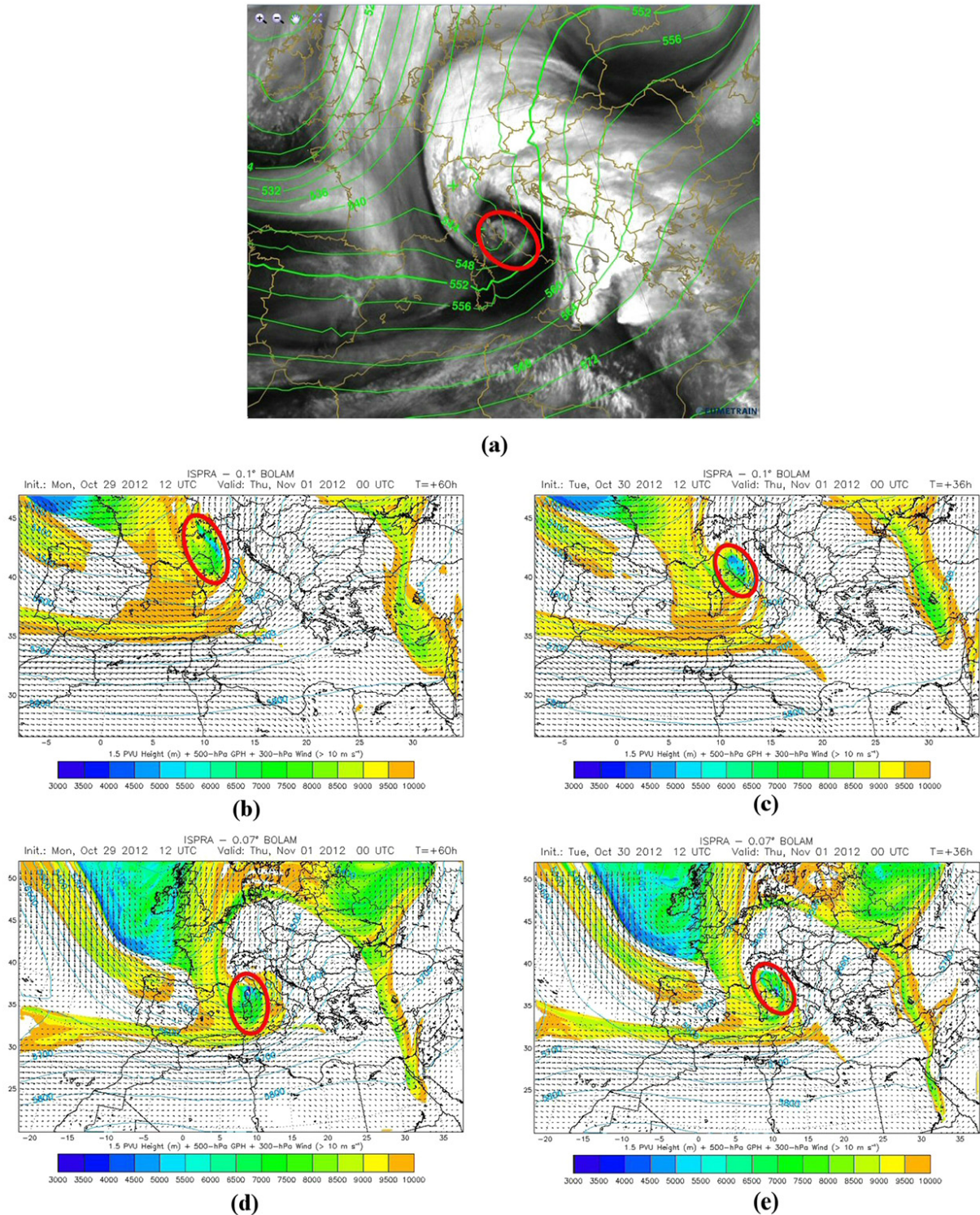


**Figure 12.** Synoptic-scale verification of BOLAM forecasts using MSG WV imagery at 00:00 UTC of 1 November 2012; the red ellipse represents the cyclone vorticity centre. (a) MSG 6.2  $\mu$ WV channel image and ECMWF analysis of 500 hPa geopotential (green contour lines); (b) 0.1° BOLAM forecast of 1.5 PVU PV isosurface height (colour shaded), 500 hPa GPH (sky blue contour lines) and 300 hPa wind stream (wind speed > 10 m s<sup>-1</sup>); the forecast initialised at 12:00 UTC of 29 October 2012. (c) As in (b), but for the forecast initialised at 12:00 UTC of 30 October 2012. (d) As in (b), but for the 0.07° BOLAM forecast. (e) As in (c), but for the 0.07° BOLAM forecast.

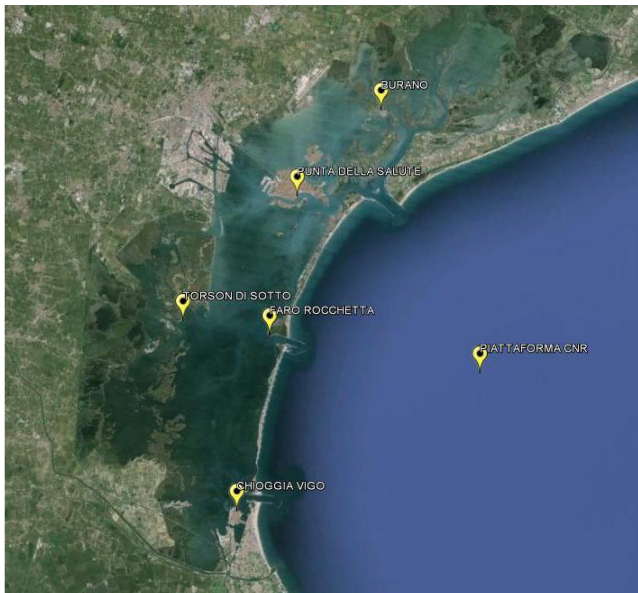


**Figure 13.** Position of the six tide-gauge instruments considered for the evaluation of the SHYFEM performance. Five stations are situated in the inner of the Venice Lagoon, whilst one is located in the Adriatic Sea.

depending on model resolution and initialisation date. The lead time anomaly is still found: the forecast delivered on 29 October is much more accurate than that delivered on 30 October, except for Burano (Fig. 16a) and Punta della Salute (Fig. 16b). In these two locations (especially in Burano), the forecast delivered on 29 October strongly overestimates the peak due to heavy north/south lagoon unbalance. The forecast delivered on 30 October underestimates the sea surge everywhere, producing the maximum error in Chioggia ( $-44$  cm; Fig. 16f). Finally, the forecast delivered on 31 October is quite accurate, despite a slight overestimation/underestimation over northerly/southerly stations (Fig. 16a, b, e).

When using the  $0.07^\circ$  BOLAM forecast (Fig. 17), the results display again the lead time anomaly, but now the forecast delivered on 30 October beats the one delivered on 31 October over the first sub-peak, where both are available. However, in the northernmost stations (Fig. 17a and b), a stronger north/south lagoon unbalance present in the former forecast results in a significant overestimation of the peak amplitude.

The reason of the unbalance effect can be easily found in the observed, strong north-northeasterly wind blowing over the lagoon in the late night of 31 October. Wind pushed the lagoon water southwards increasing the sea level difference in the north–south direction. Thus, the behaviour of the SHYFEM error can be easily related to the error associated with the forecast of surface winds provided by the different BOLAM simulations. To further clarify this issue, the 10 m wind field observed over NEI at 00:00 UTC

of 1 November – calculated by the Environmental Agency of the Veneto Region (ARPA Veneto) using the CALifornia METeorological model (CALMET; Sansone et al., 2005) – is compared against the corresponding BOLAM simulations obtained with different initialisations (see Fig. 18). The  $0.1^\circ$  BOLAM initialised using the 12:00 UTC IFS run on 30 October (Fig. 18c) and the  $0.07^\circ$  BOLAM initialised using the 12:00 UTC IFS run on 31 October (Fig. 18e), which are associated with the minimum north/south lagoon unbalance (see Figs. 16 and 17), predict correctly the northeasterly winds over the lagoon. Instead, significant cross-lagoon winds are predicted by the  $0.1^\circ$  BOLAM initialised using the 12:00 UTC IFS run on 29 October (Fig. 18b) and by the  $0.07^\circ$  BOLAM initialised using the 12:00 UTC IFS run on 30 October (Fig. 18f), which are consistently associated with the maximum north/south lagoon unbalance (see Figs. 16 and 17).

Figure 18 is also very effective in showing how much the dynamically relevant differences in the mesoscale cyclone shown in Fig. 12 can affect key features in forecasting both the rainfall and the sea surge event, namely: the veering of Scirocco flow over the northern Adriatic Sea (and its timing, not shown); the front sharpness; the wind speed and direction inside and outside the lagoon (which depend on the trajectory of the surface pressure minimum in the area); and the fine structure of the cyclone.

Finally, forecast verification of the storm surge contribution was also performed in Piattaforma (not shown). No tidal residual comparison is possible at the lagoon stations since only the total water level is available there. During IOP16, the observed tidal residual oscillates between 35 and 65 cm, with a period of 20–22 h (seiches). For each NWP model, the forecast error is mainly due to a phase shift in the prediction of this fluctuation. However, since the astronomical tide contribution is dominant in this event, the tidal residual forecast error is relevant only when it occurs in correspondence to the astronomical tide peak on 27 October. The results for the IOP18 event show, instead, that the storm surge is dominant with respect to the astronomical tide contribution. The observed storm surge displays a high (ca. 110 cm), long-lasting (ca. 36 h) single peak, and the model errors are mostly due to the underestimation of this peak. These results confirm the above-discussed outcomes of the tidal forecast verification.

The verification results can be summarised as follows. On IOP16, the SHYFEM performance improves by increasing the resolution of the meteorological forcing. As expected, the most recent forecast is always the best one. On IOP18, even if the BOLAM-driven runs are more skilful than the IFS-driven ones, the SHYFEM accuracy in predicting the sea level peak depends in a nontrivial way on meteorological input resolution, initial date, and geographical location. This is the combined effect of the low predictability of the IOP18 cyclone and the high sensitivity of tidal forecast to details of the meteorological fields.

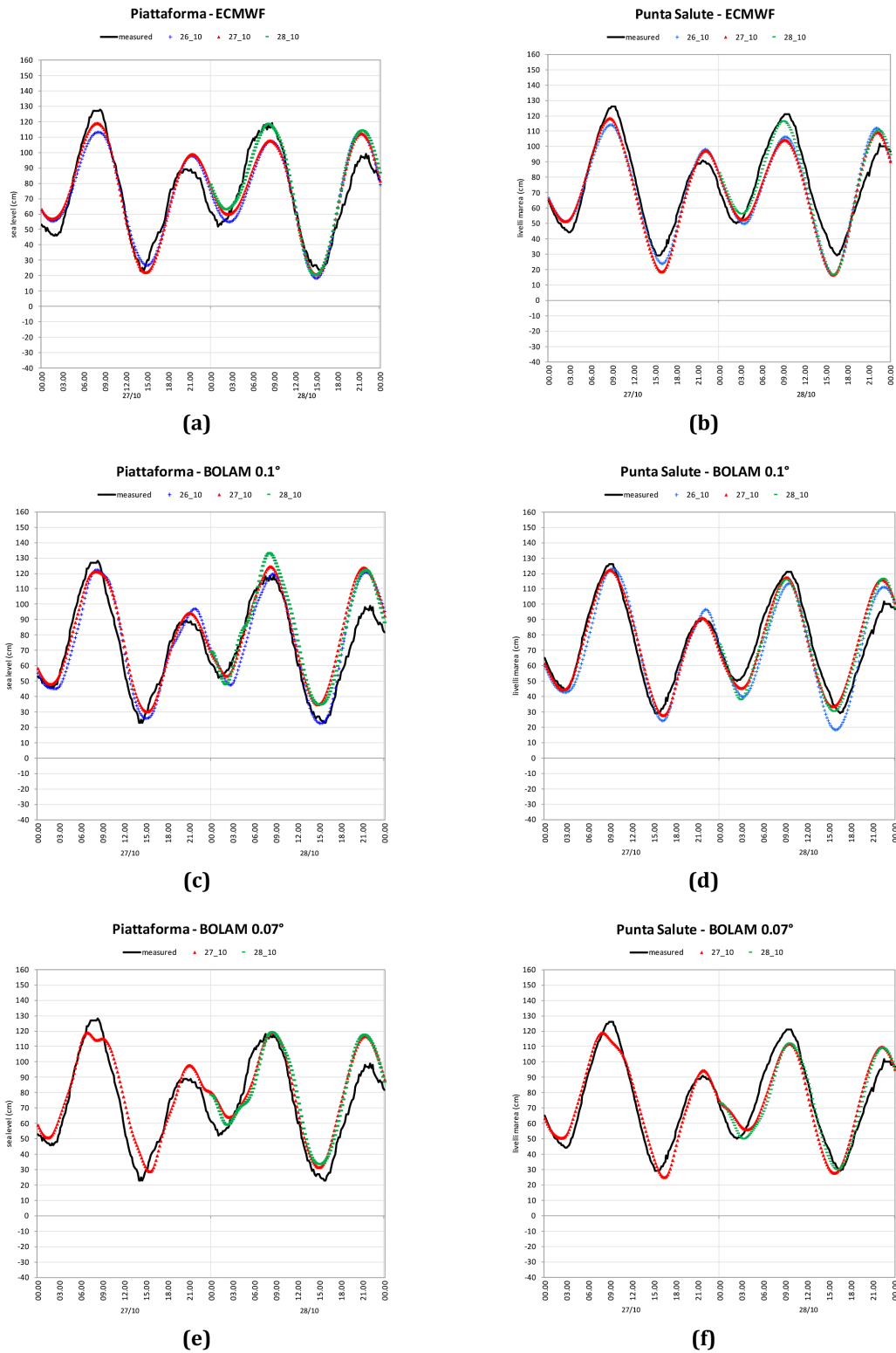


**Figure 14.** Comparison for IOP16 between the SHYFEM forecasts and the sea level observations registered at Piattaforma and Punta della Salute. Time in CET (UTC+1). Meteorological forcing by: (a and b) ECMWF IFS forecasts from 26 to 28 October; (c and d) 0.1° BOLAM forecasts from 26 to 28 October; (e and f) 0.07° BOLAM forecasts from 27 to 28 October.

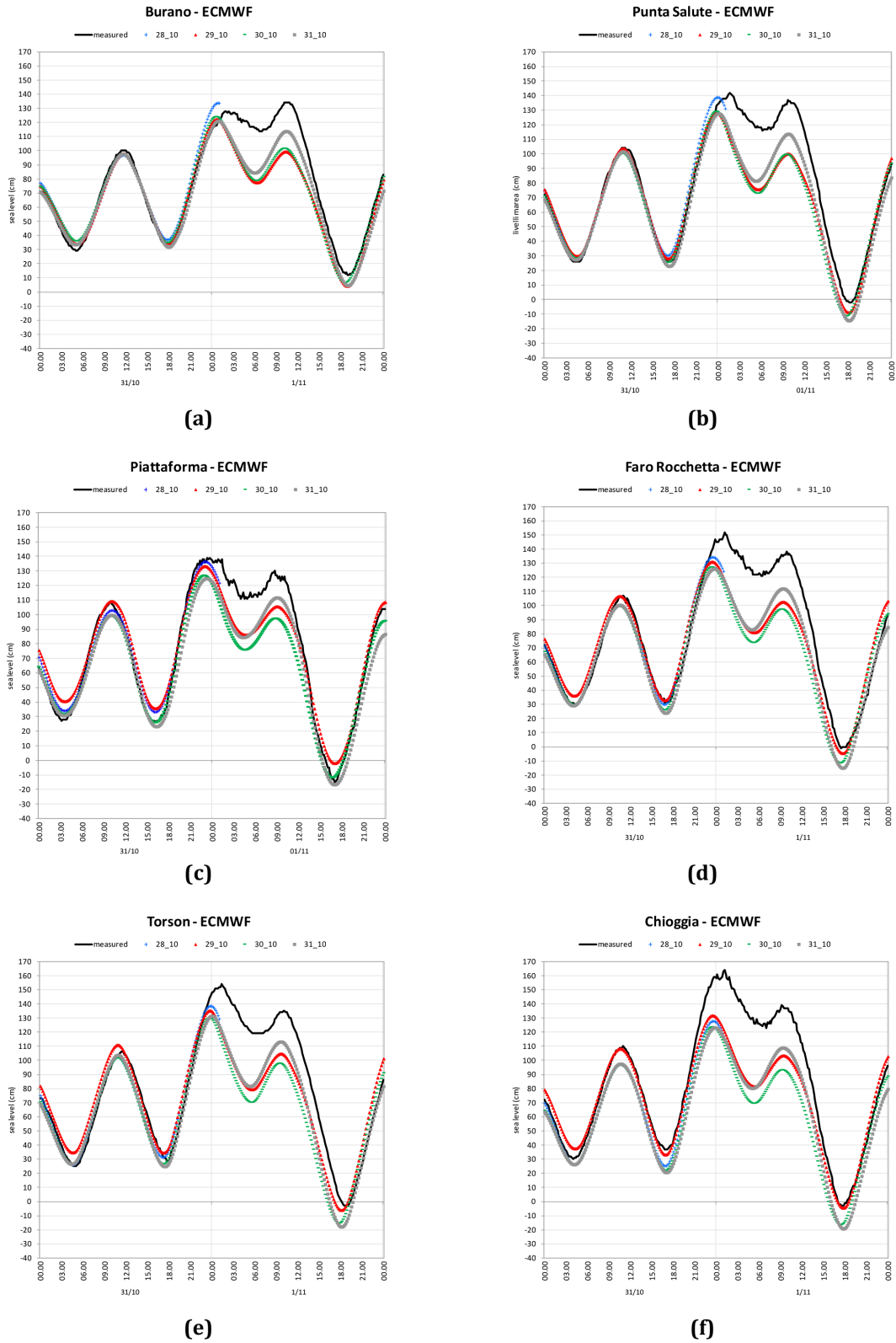


**Figure 15.** Comparison for IOP18 between the ECMWF IFS-forced SHYFEM forecasts and the sea level observations registered at the six considered tide-gauge instruments, with meteorological forecast forcing from 28 to 31 October: (a) Burano; (b) Punta della Salute; (c) Piattaforma; (d) Faro Rocchetta; (e) Torson; (f) Chioggia.

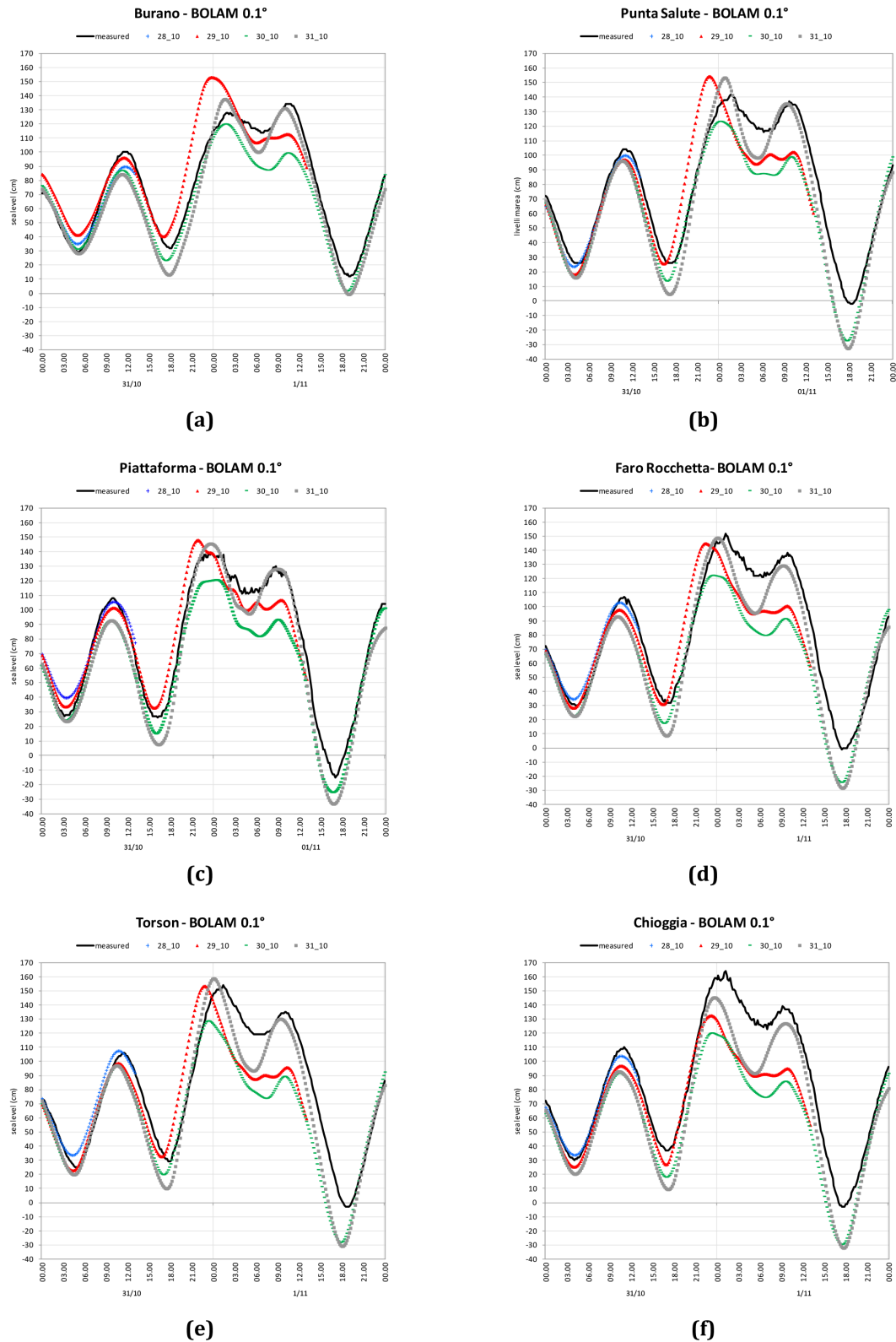


**Figure 16.** As in Fig. 15, but with the meteorological forecast forcing provided by the 0.1° BOLAM: (a) Burano; (b) Punta della Salute; (c) Piattaforma; (d) Faro Rocchetta; (e) Torson; (f) Chioggia.

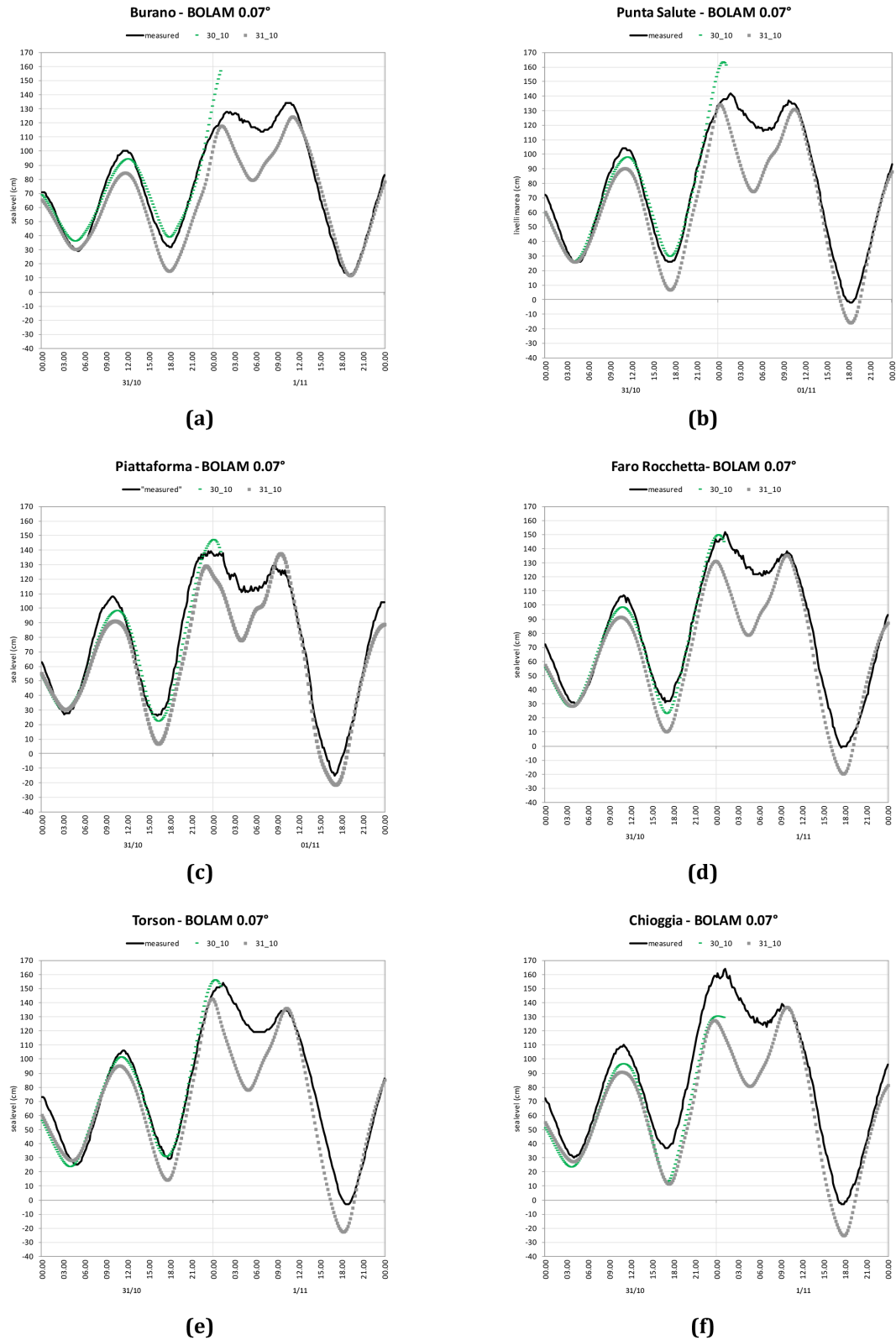


**Figure 17.** As in Fig. 15, but with the meteorological forecast forcing provided by the 0.07° BOLAM from 30 to 31 October: (a) Burano; (b) Punta della Salute; (c) Piattaforma; (d) Faro Rocchetta; (e) Torson; (f) Chioggia.

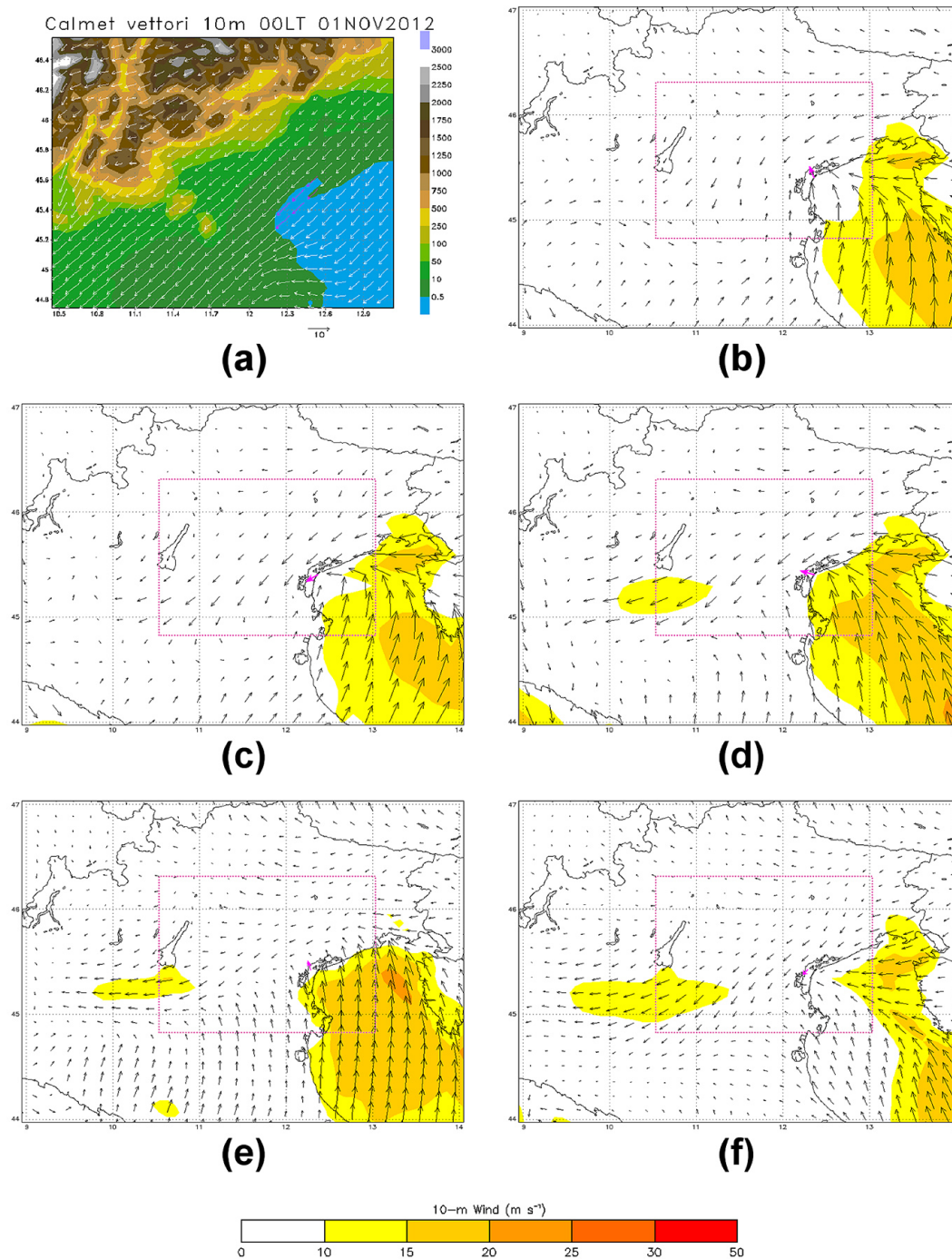


**Figure 18.** Observed and forecast 10 m wind field over NEI at 00:00 UTC of 1 November 2012. (a) The CALMET wind analysis – courtesy of ARPA Veneto; (b)  $0.1^\circ$  BOLAM forecast initialised at 12:00 UTC of 28 October 2012. (c) As in (b), but for the forecast initialised at 12:00 UTC of 29 October 2012; (d) As in (b), but for forecast initialised at 12:00 UTC of 30 October 2012; (e)  $0.07^\circ$  BOLAM forecast initialised at 12:00 UTC of 29 October 2012; (f) As in (e), but for the forecast initialised at 12:00 UTC of 30 October 2012.

## 5 Conclusions

Evaluating the performance of an integrated meteo-marine modelling system, such as SIMM, is a demanding task since forecasts have to be verified at any model stage, and the results should be inter-related to provide a whole picture of the system skill and value. In addition, the assessment of such a system in forecasting high impact events is essential for any operational centre involved in predicting and monitoring natural hazards. In this context, forecast verification is also relevant to determine in advance whether modifications of the system configuration lead to performance improvements.

The first HyMeX SOP experience gives the opportunity (and the necessary observations) to perform an intercomparison study of two different configurations of SIMM, namely the operational and the ad hoc implemented for HyMeX. Despite an apparent similarity of weather patterns and surface effects, the IOP16 and IOP18 events are characterised by different predictability: the results indicate that the cyclone responsible for the latter event is much less predictable than that involved in the former one.

The QPF intercomparison displays an objective added value of MOLOCH forced by the 0.07° BOLAM in predicting the two most relevant rainfall episodes. In the IOP16 LT event, a well-described, unstable flow over orography makes model resolution the key issue for a good forecast. This is partially true also for the IOP18 NEI event. However, squall lines developing over sea in the warm sector, as the ones involved in both IOP CI events, are less able to take benefit from the resolution increase. In fact, when the model resolution is increased, the forecast rain bands tend to be more realistic but not necessarily more accurate. In addition, the IOP18 results show that the lack of predictability of the involved cyclone is a key factor that affects the precipitation forecast quality. The rainfall patterns predicted over NEI are sensitive to ICs, and forecasts obtained by changing the model configuration and initial date display a significant spread concerning cyclone trajectory and intensity. The large-scale discrepancies among the different forecasts induce, as a consequence, differences in the prediction of local dynamical processes, which have a key role in triggering precipitation over NEI.

The study is completed by a statistical verification of the MOLOCH QPFs during 3 months, including the first HyMeX SOP devoted to the monitoring of high precipitation events. This represents the first objective evaluation of the ISPRA version of the non-hydrostatic MOLOCH model. This is the starting point to assess the impact (and improvement, if any) on forecast performance of some planned modifications of model configurations – in particular the extension of the model domain to include Italy and the conterminous seas. At a first glance, the categorical scores are comparable with those obtained for the other two versions of MOLOCH used by the CNR-ISAC for the HyMeX SOPs.

The tidal forecast verification clearly displays, for both events, better results when SHYFEM is forced with the forecasts provided by the two BOLAM configurations, rather than ECMWF IFS fields. Concerning the intercomparison between the two different BOLAM initialisations, the different predictability of the two examined weather systems still emerges as a crucial issue. For IOP16, both initialisations provide very good results, with some small differences. For IOP18, the differences in the tide peak forecast due to the use of the two different BOLAM versions are of the same order of magnitude as the differences among runs with different initial dates (the most recent forecast being not always the best one) or the small-scale, latitude-dependent systematic errors. A wrong surface wind prediction over the Venice Lagoon introduces latitude-dependent systematic errors that do not depend from the overall sea elevation error (that can be assumed to be represented by the error at the CNR Piattaforma).

IOP18 cannot be regarded as a negligible exception. An association between relatively high *acqua alta* events and highly chaotic weather systems was found in a recent study by Mel and Lionello (2014). To deal with chaos, they proposed to apply an ensemble prediction system (EPS; Buizza et al., 2005) strategy to the operational storm surge forecasting task over the Venice Lagoon. Over a sample of 10 events, it was found that the most intense ones were associated to large EPS spread. Even without a suitable EPS forecasting system, the large spread displayed by the “pool” of SHYFEM forecasts generated with different initial dates and model configurations can be regarded as an indicator of the low predictability of the IOP18 event. In our operational context, this sort of time-lagged multi-model ensemble (see, e.g., García-Moya et al., 2011; Jie et al., 2014) should provide hints about the predictability of forthcoming events and, consequently, about the forecast reliability. However, in order to provide probabilistic forecasts, a probability measure should be associated to each ensemble member. Thus, in our future activities, it is planned to build up a long-term operational statistics to achieve this goal.

Finally, the precipitation and tide forecast verification results display the added value provided by high-resolution BOLAM-MOLOCH suite into the SIMM, encouraging us to make it fully operational. The outcome about predictability of intense *acqua alta* events suggests, however, to maintain operational as well as the SHYFEM configurations forced by the lower-resolution meteorological forecasts, thereby aiming at developing and testing a time-lagged multi-model ensemble.

*Acknowledgements.* The authors are grateful to Marco Cordella and Devis Canesso (ISPRA) and Marco Bajo (CNR-ISMAR) for providing useful information on the SHYFEM simulations and for making available data from the RMLV tide gauges and the Venice Municipality tide gauge. Special thanks go to Maria Sansone and Massimo Enrico Ferrario (ARPAV) for the CALMET analysis.

The Italian Air Force Meteorological Service is acknowledged for providing the ECMWF-IFS data used to initialise the two SIMM configurations. KNMI and EUTMESAT are acknowledged for the synoptic analysis charts and the MSG 6.2  $\mu$ WV channel image, respectively. The authors also acknowledge the HyMeX partners for supplying the rain gauge data used in this study and the HyMeX database teams (ESPRI/IPSL and SEDOO/Observatoire Midi-Pyrénées) for their help in accessing the data. Special thanks go to the Italian HyMeX Group for the excellent and fruitful collaboration during the first SOP campaign and beyond.

Edited by: E. Richard

Reviewed by: two anonymous referees

## References

- Bajo, M., Zampato, L., Umgiesser, G., Cucco, A., and Canestrelli, P.: A finite element operational model for storm surge prediction in Venice, *Estuar. Coast. Shelf. S.*, 75, 236–249, doi:10.1016/j.ecss.2007.02.025, 2007.
- Bajo, M., Coraci, E., and Umgiesser, G.: Sviluppo di un sistema operativo, basato su tecniche di assimilazione dati in tempo reale, per la previsione della marea reale presso le stazioni di riferimento della Rete mareografica della laguna di Venezia e del litorale Nord-Adriatico (RMLV), *Rapporto tecnico finale, CNR-ISMAR*, 34 pp., 2012.
- Booij, N., Ris, R. C., and Holthuijsen, L. H.: A third-generation wave model for coastal regions, Part I: Model description and validation, *J. Geophys. Res.*, 104, 7649–7666, 1999.
- Brier, B. G. and Allen, R. A.: Verification of weather forecast, in: *Compendium of Meteorology*, edited by: Malone, T. F., *Am. Meteorol. Soc.*, Boston, MA, 841–848, 1951.
- Buizza, R., Houtekamer, P. L., Pellerin, G., Toth, Z., Zhu, Y., and Wei, M.: A comparison of the ECMWF, MSC, and NCEP Global Ensemble Prediction Systems, *Mon. Weather Rev.*, 133, 1076–1097, 2005.
- Buzzi, A., Fantini, M., Malguzzi, P., and Nerozzi, F.: Validation of a limited area model in cases of Mediterranean cyclogenesis: Surface fields and precipitation scores, *Meteorol. Atmos. Phys.*, 53, 53–67, 1994.
- Casaioli, M., Mariani, S., Malguzzi, P., and Speranza, A.: Factors affecting the quality of QPF: A multi-method verification of multi-configuration BOLAM reforecasts against MAP D-PHASE observations, *Meteor. Appl.*, 20, 150–163, doi:10.1002/met.1401, 2013.
- Casaioli, M., Catini, F., Inghilesi, R., Malguzzi, P., Mariani, S., Lanucara, P., and Orasi, A.: Towards an operational forecasting system for the meteorological, hydrological and marine conditions in Mediterranean coastal areas, *Adv. Res. Sci.*, 11, 11–23, 2014.
- Cavaleri, L.: The oceanographic tower Acqua Alta: more than a quarter of a century of activity, *Nuovo Cimento*, 22, 1–111, 1999.
- Coraci, E.: Valutazione su un anno di operatività del modello deterministico per la previsione della marea reale presso le stazioni di riferimento della Rete mareografica della laguna di Venezia e del litorale Nord-Adriatico, available at: <http://www.venezia.isprambiente.it/ricerche>, last access: 29 July 2014.
- Cordella, M.: Storm surge forecast activities in the Northern Adriatic Sea and in the lagoons, *Storm Surge Networking Forum 2013*, eSurge project, Venice, Italy, 18–20 November 2013, available at: <http://www.venezia.isprambiente.it/ricerche> (last access: 13 January 2014), 2013.
- Crosato, F.: Eventi di marea eccezionale in alto Adriatico, *Rapporto ISPRA Venezia n. 1/2012 – Analisi eventi novembre 2012*, available at: [http://www.venezia.isprambiente.it/ispra/index.php?action=download&upload\\_id=151891](http://www.venezia.isprambiente.it/ispra/index.php?action=download&upload_id=151891) (last access: 26 November 2013), 2012.
- Drobinski, P., Ducrocq, V., Alpert, P., Anagnostou, E., Béranger, K., Borga, M., Braud, I., Chanzy, A., Davolio, S., Delrieu, G., Estournel, C., Filali Boubrahmi, N., Font, J., Grubisic, V., Gualdi, S., Homar, V., Ivancan-Picek, B., Kottmeier, C., Kotroni, V., Lagouvardos, K., Lionello, P., Llasat, M. C., Ludwig, W., Lutoff, C., Mariotti, A., Richard, E., Romero, R., Rotunno, R., Roussot, O., Ruin, I., Somot, S., Taupier-Letage, I., Tintore, J., Uijlenhoet, R., and Wernli, H.: HyMeX, a 10-year multidisciplinary program on the Mediterranean water cycle, *B. Am. Meteorol. Soc.*, 95, 1063–1082, doi:10.1175/BAMS-D-12-00242.1, 2014.
- Ducrocq, V., Braud, I., Davolio, S., Ferretti, R., Flamant, C., Jansa, A., Kalthoff, N., Richard, E., Taupier-Letage, I., Ayrat, P.-A., Belamari, S., Berne, A., Borga, M., Boudevillain, B., Bock, O., Boichard, J.-L., Bouin, M.-N., Bousquet, O., Bouvier, C., Chigiato, J., Cimini, D., Corsmeier, U., Coppola, L., Cocquerez, P., Defer, E., Delanoë, J., Di Girolamo, P., Doerenbecher, A., Drobinski, P., Dufournet, Y., Fourrié, N., Gourley, J. J., Labatut, L., Lambert, D., Le Coz, J., Marzano, F. S., Molinié, G., Montani, A., Nord, G., Nuret, M., Ramage, K., Rison, B., Roussot, O., Frédérique Said, F., Schwarzenboeck, A., Testor, P., Baelen, J. V., Vincendon, B., Aran, M., and Tamayo, J.: HyMeX-SOP1, the field campaign dedicated to heavy precipitation and flash flooding in the northwestern Mediterranean, *B. Am. Meteorol. Soc.*, 95, 1083–1100, doi:10.1175/BAMS-D-12-00244.1, 2014.
- Ferla, M.: Il Sistema ISPRA di previsione dei fenomeni di storm surge in Alto Adriatico, *Workshop “I Sistemi multirischio in Italia”*, Bologna, Italy, 25 ottobre 2013, available at: <http://www.venezia.isprambiente.it/ricerche> (last access: 13 January 2014), 2013.
- Ferretti, R., Pichelli, E., Gentile, S., Maiello, I., Cimini, D., Davolio, S., Miglietta, M. M., Panegrossi, G., Baldini, L., Pasi, F., Marzano, F. S., Zinzi, A., Mariani, S., Casaioli, M., Bartolini, G., Loglisci, N., Montani, A., Marsigli, C., Manzato, A., Pucillo, A., Ferrario, M. E., Colaiuda, V., and Rotunno, R.: Overview of the first HyMeX Special Observation Period over Italy: observations and model results, *Hydrol. Earth Syst. Sci.*, 18, 1953–1977, doi:10.5194/hess-18-1953-2014, 2014.
- García-Moya, J.-A., Callado, A., Escribà, P., Santos, C., Santos-Muñoz, D., and Simarro, A.: Predictability of short-range forecasting: a multimodel approach, *Tellus*, 63, 550–563, 2011.
- Gilleland, E.: Testing competing precipitation forecasts accurately and efficiently: the spatial prediction comparison test, *Mon. Weather Rev.*, 141, 340–355, 2013.
- Inghilesi, R., Catini, F., Bellotti, G., Franco, L., Orasi, A., and Corsini, S.: Implementation and validation of a coastal forecasting system for wind waves in the Mediterranean Sea, *Nat. Hazards Earth Syst. Sci.*, 12, 485–494, doi:10.5194/nhess-12-485-2012, 2012.

- Jansa, A., Alpert, P., Arbogast, P., Buzzi, A., Ivancan-Picek, B., Kotroni, V., Llasat, M. C., Ramis, C., Richard, E., Romero, R., and Speranza, A.: MEDEX: a general overview, *Nat. Hazards Earth Syst. Sci.*, 14, 1965–1984, doi:10.5194/nhess-14-1965-2014, 2014.
- Jie, W., Wu, T., Wang, J., Li, W., and Liu, X.: Improvement of 6–15 day precipitation forecasts using a time-lagged ensemble method, *Adv. Atmos. Sci.*, 31, 293–304, 2014.
- Jolliffe, I. T. and Stephenson, D. B. (Eds.): *Forecast Verification: A Practitioner's Guide in Atmospheric Science*, 2nd edition, John Wiley & Sons Ltd., Chichester, 292 pp., 2011.
- Jurčec, V.: On mesoscale characteristics of Bora conditions in Yugoslavia, *Pure Appl. Geophys.*, 119, 640–657, 1981.
- Lanciani, A., Mariani, S., Casaioli, M., Accadia, C., and Tartaglione, N.: A multiscale approach for precipitation verification applied to the FORALPS case studies, *Adv. Geosci.*, 16, 3–9, doi:10.5194/adgeo-16-3-2008, 2008.
- Malguzzi, P. and Tartaglione, N.: An economical second-order advection scheme for numerical weather prediction, *Q. J. Roy. Meteorol. Soc.*, 125, 2291–2303, 1999.
- Malguzzi, P., Grossi, G., Buzzi, A., Ranzi, R., and Buizza, R.: The 1996 “century” flood in Italy. A meteorological and hydrological revisit, *J. Geophys. Res.*, 111, D24106, doi:10.1029/2006JD007111, 2006.
- Mariani, S., Casaioli, M., Lanciani, A., Flavoni, S., and Accadia, C.: QPF performance of the updated SIMM forecasting system using reforecasts, *Meteor. Appl.*, doi:10.1002/met.1453, online first, 2014.
- Mass, C. F., Owens, D., Westrick, K., and Colle, A. B.: Does increasing horizontal resolution produce more skilful forecasts?, *B. Am. Meteorol. Soc.*, 83, 407–430, 2002.
- Mel, R. and Lionello, P.: Storm Surge Ensemble Prediction for the city of Venice, *Wea. Forecasting*, 29, 1044–1057, 2014.
- Romero, R.: Application of Factor Separation to heavy rainfall and cyclogenesis: Mediterranean examples, in: *Factor Separation in the Atmosphere, Applications and Future Prospects*, edited by: Alpert, P. and Sholokhman, T., Cambridge University Press, Cambridge, UK, 87–119, 2011.
- Rossa, A., Nurmi, P., and Ebert, E. E.: Overview of methods for the verification of quantitative precipitation forecasts, in: *Precipitation: Advances in Measurement, Estimation and Prediction*, edited by: Michaelides, S. C., Springer-Verlag, New York, NY, 419–452, 2008.
- Sansone, M., Pernigotti, D., and Ferrario, M. E.: Application of CALMET model to the the Veneto region, with particular attention to the shoreline, using offshore data for initialization, in: *Proceedings of the 1st International Conference on Harbours and Air Quality*, Genoa, Italy, 15–17 June 2005.
- Speranza, A., Buzzi, A., Trevisan, A., and Malguzzi, P.: A theory of deep cyclogenesis in the lee of the Alps. Part I: Modifications of baroclinic instability by localized topography, *J. Atmos. Sci.*, 42, 1521–1535, 1985.
- Speranza, A., Accadia, C., Casaioli, M., Mariani, S., Monacelli, G., Inghilesi, R., Tartaglione, N., Ruti, P. M., Carillo, A., Bargagli, A., Pisacane, G., Valentinotti, F., and Lavagnini, A.: POSEIDON: An integrated system for analysis and forecast of hydrological, meteorological and surface marine fields in the Mediterranean area, *Nuovo Cimento*, 27C, 329–345, 2004.
- Speranza, A., Accadia, C., Mariani, S., Casaioli, M., Tartaglione, N., Monacelli, G., Ruti, P. M., and Lavagnini, A.: SIMM: An integrated forecasting system for the Mediterranean area, *Meteorol. Appl.*, 14, 337–350, 2007.
- The SWAN Team: *SWAN Technical Manual, SWAN Cycle III*, Delft University of Technology, available at: <http://swanmodel.sourceforge.net/>, last access: 3 April 2014.
- The Wamdi Group: *The WAM model—A third generation ocean wave prediction model*, *J. Phys. Oceanogr.*, 18, 1776–1810, 1988.
- Umgiesser, G., Melaku Canu, D., Cucco, A., and Solidoro, C.: A finite element model for the Venice Lagoon. Development, set up, calibration and validation, *J. Mar. Sys.*, 51, 123–145, 2004.
- Weygandt, S. S., Loughe, A. F., Benjamin, S. G., and Mahoney, J. L.: Scale sensitivities in model precipitation skill scores during IHOP, in: *Proceedings of 22nd Conference on Severe Local Storms*, Hyannis, MA, 4–8 October 2004, *Am. Meteorol. Soc.*, Boston, MA, 16A.8, 2004.
- Zampato, L., Umgiesser, G., and Zecchetto, S.: Sea level forecasting in Venice through high resolution meteorological fields, *Estuar. Coast. Shelf. S.*, 75, 223–235, doi:10.1016/j.ecss.2007.02.024, 2007.